cmgh
CELLULAR AND MOLECULAR GASTROENTEROLOGY AND HEPATOLOGY

ORIGINAL RESEARCH

The miR-23b/27b/24-1 Cluster Inhibits Hepatic Fibrosis by Inactivating Hepatic Stellate Cells

Lin-Yan Wan,[1,2,3,4,5,*] Hu Peng,[1,2,3,6,*] Yi-Ran Ni,[1,2,3,*] Xue-Ping Jiang,[1,2,3,7,*] Jiao-Jiao Wang,[1,2] Yan-Qiong Zhang,[1,2,3] Lan Ma,[1,2,3,4] Rui Li,[1,2,3] Lin Han,[5] Yong Tan,[1,2,3] Jun-Ming Li,[5] Wen-Li Cai,[1,2] Wen-Fang Yuan,[1,2,3] Jia-Jie Liang,[1,2,3] Lu Huang,[1,2,3] Xu Wu,[1,2] Quan Zhou,[5] Qi-Ni Cheng,[1,2,3] Xue Yang,[1,2,3] Meng-Yuan Liu,[1,2,3] Wen-Bing Ai,[1,2,6] Chang-Bai Liu,[1,2,3] Hongbing Zhang,[1,2,3,4,5] and Jiang-Feng Wu[1,2,3,4,5,6]

[1]Medical College, [2]Institute of Organ Fibrosis and Targeted Drug Delivery, [3]Hubei Key Laboratory of Tumor Microenvironment and Immunotherapy, [5]Institute of Organ Fibrosis and Targeted Drug Delivery, The People's Hospital, China Three Gorges University, Yichang, China; [4]State Key Laboratory of Medical Molecular Biology, Department of Physiology, Institute of Basic Medical Sciences, School of Basic Medicine, Chinese Academy of Medical Sciences, Peking Union Medical College, Beijing, China; [6]Department of Surgery, The Yiling Hospital of Yichang, Yichang, China; [7]Department of Oncology II, The Central Hospital of Enshi Autonomous Prefecture, Enshi Clinical College of Wuhan University, Enshi, Hubei, China

SUMMARY

Increasing the microRNA-23b/27b/24-1 level through intravenous delivery of miR-23b/27b/24-1 lentivirus ameliorated mouse hepatic fibrosis. Mechanistically, the miR-23b/27b/24-1 cluster directly targeted messenger RNAs of 5 secretory profibrotic genes (TGF-β2, Gremlin1, LOX, Itgα2, and Itgα5) in hepatic stellate cells.

BACKGROUND & AIMS: Hepatic fibrosis is characterized by hepatic stellate cell (HSC) activation and transdifferentiation-mediated extracellular matrix (ECM) deposition, which both contribute to cirrhosis. However, no antifibrotic regimen is available in the clinic. microRNA-23b/27b/24-1 cluster inhibition of transforming growth factor-β (TGF-β) signaling during hepatic development prompted us to explore whether this cluster inhibits HSC activation and hepatic fibrosis.

METHODS: Experimental fibrosis was studied in carbon tetrachloride (CCl_4)-treated C57BL/6 mice. After administration of miR-23b/27b/24-1 lentivirus or vehicle, animals were euthanized for liver histology. In primary rat HSC and HSC-T6, the anti-fibrotic effect of miR-23b/27b/24-1 cluster was furtherly investigated by RNA-sequencing, luciferase reporter assay, western blotting and bioinformatic means.

RESULTS: In this study, we showed that increasing the miR-23b/27b/24-1 level through intravenous delivery of miR-23b/27b/24-1 lentivirus ameliorated mouse hepatic fibrosis. Mechanistically, the miR-23b/27b/24-1 cluster directly targeted messenger RNAs, which reduced the protein expression of 5 secretory profibrotic genes (*TGF-β2*, *Gremlin1*, *LOX*, *Itgα2*, and *Itgα5*) in HSCs. Suppression of the TGF-β signaling pathway by down-regulation of TGF-β2, Itgα2, and Itgα5, and activation of the bone morphogenetic protein signaling pathway by inhibition of Gremlin1, decreased extracellular matrix secretion of HSCs. Furthermore, down-regulation of LOX expression softened the ECM. Moreover, a reduction in tissue inhibitors of metalloproteinase 1 expression owing to weakened TGF-β signaling increased ECM degradation.

CONCLUSIONS: Hepatic overexpression of the miR-23b/27b/24-1 cluster blocked hepatic fibrosis and may be a novel therapeutic regimen for patients with hepatic fibrosis. *(Cell Mol Gastroenterol Hepatol 2022;13:1393–1412; https://doi.org/10.1016/j.jcmgh.2022.01.016)*

Keywords: miR-23b/27b/24-1 Cluster; TGF-β2; Gremlin1; LOX; Itgα2/5; Hepatic Stellate Cells; Hepatic Fibrosis.

Multiple pathogens cause liver injury and inflammation, trigger repair mechanisms, and lead to fibrosis, cirrhosis, and cancer.[1] Because of a repeated chronic liver inflammation–wound healing response, hepatic fibrosis is the intermediate stage between hepatitis and cirrhosis. The primary characteristic of hepatic fibrosis is the activation and subsequent transdifferentiation of hepatic stellate cells (HSCs), fat-storing cells that reside in the

*Authors share co-first authorship.

Abbreviations used in this paper: **ALK5, anaplastic lymphoma kinase 5; BMP, bone morphogenetic protein; CTGF, connective tissue growth factor; DMEM, Dulbecco's modified Eagle medium; ECM, extracellular matrix; GO, Gene Ontology; HSC, hepatic stellate cell; ITG, integrin; KEGG, Kyoto Encyclopedia Genes and Genomes; LOX, lysyl oxidase; LOXL, lysyl oxidase–like proteins; LV-Puro, lentivirus-puro; miRNA, microRNA; mRNA, messenger RNA; miR-23b/27b/24-1, microRNA-23b/27b/24-1; MMP, matrix metalloproteinase; pCDH, pCDH-CMV-MCS-EF1; PCR, polymerase chain reaction; pMIR-Luc, pMIR-REPORT™ Luciferase; PPI, protein–protein interaction; RNA-seq, RNA sequencing; Smad, SMAD family member; TGF- β, transforming growth factor-β; TIMP, tissue inhibitors of metalloproteinase; TPEF/SHG, second harmonic generation/2-photon excitation fluorescence; UTR, untranslated region.**

Most current article

2352-345X
https://doi.org/10.1016/j.jcmgh.2022.01.016

space of Disse between hepatocytes and sinusoidal endothelial cells.[2] In addition to HSC activation and transdifferentiation, in hepatic fibrosis, extracellular matrix (ECM) deposition and cross-linking increase, and ECM degradation decreases,[3] resulting in excessive ECM in the liver that eventually can lead to distorted liver histologic architecture and impaired liver function.[4]

Six classes of hepatic fibrosis–related genes, including ECM-related genes, TGF-β superfamily members, *ITG*s, *MMP*s, *TIMP*s, and *LOX*,[4] participate in hepatic fibrosis. Of the 28 types of ECM collagens, the levels of type I, III, IV, V, VI, X, and XVIII collagens increase during hepatic fibrosis progression.[5] Most TGF-β superfamily members, including TGF-β proteins, bone morphogenetic proteins (BMPs), activins, and differentiation factors, are liver fibrosis–related proteins. Among these proteins, TGF-β proteins and BMPs exert opposite effects during hepatic fibrogenesis.[6] On the one hand, the activated TGF-β signaling pathway promotes HSC activation. Ligation of TGF-β receptors with TGF-β leads to phosphorylation of SMAD family member 2/3 (Smad2/3), which binds to Smad4 and is shuttled into the nucleus to promote the expression of hepatic fibrosis agonists, such as *Gremlin1*, *collagen*, and *TIMP* genes.[7] On the other hand, BMPs promote Smad1/5/8 phosphorylation and, along with Smad4, subsequent nuclear translocation to inhibit HSC activation. The activated TGF-β signaling pathway suppresses the BMP signaling pathway through Smad6 action, and the activated BMP signaling pathway suppresses the TGF-β signaling pathway through Smad7 action.[8] The human ITG family consists of cell adhesion receptors, which have 18 α-subunits and 8 β-subunits in combinations that form 24 different members.[9] ITGα1β1, α2β1, α5β1, α11β1, αVβ1, αVβ3, αVβ5, and αVβ8 are expressed on HSCs. ITGs and TGF-β proteins promote HSC activation and increase ECM secretion.[10] Human MMPs comprise 23 enzymes, among which 13 MMPs (MMP-1, MMP-2, MMP-3, MMP-7, MMP-8, MMP-9, MMP-10, MMP-12, MMP-13, MMP-14, MMP-16, MMP-19, and MMP-24) attenuate hepatic fibrosis by degrading the ECM.[11] These MMPs are inhibited by at least 1 of TIMP, TIMP-1, TIMP-2, TIMP-3, and/or TIMP-4. Enhanced TIMP or decreased MMP expression is a principal cause of hepatic fibrosis.[12] The LOX family consists of LOX and 4 LOX-like proteins (LOXL-1, -2, -3, and -4).[13] Among these proteins, LOX,[14] LOXL-1, LOXL-2,[15] and LOXL-3 resist fibrosis reversal by inducing covalent fibrillar collagen and elastin cross-linking.

Because of the complexity of its pathogenesis, hepatic fibrosis is extremely difficult to treat. To date, no reliable antifibrotic regimen has been approved by the Food and Drug Administration for clinical practice.[4,16] Expelling evil and strengthening the body and seeking the good and avoiding the bad are strategies to treat diseases with complicated pathogenesis. Suppression of hepatic fibrosis agonists and enhancement of hepatic fibrosis antagonists is a rational approach for hepatic fibrosis treatment. The human microRNA-23b/27b/24-1 cluster is located between introns 14 and 15 in chromosome 9 open reading frame 3 at 9q22.32. The miR-23b/27b/24-1 cluster belongs to a heterosequence seed cluster with a higher degree of evolutionary conservation, and the evolutionary mechanism is based on functional co-adaptation selection interference.[17] The heterosequence seed clusters are thought to target the same messenger RNA (mRNA) or different mRNAs of proteins in the same pathway to exert linking functions or activate functionally related molecules.[18] Most of the studies on the miR-23b/27b/24-1 cluster have focused on the roles of individual microRNAs (miRNAs) in regulating specific targets.[19,20] However, the potentially coordinated effects of the miR-23b/27b/24 cluster on diseases are not fully understood.

In this study, we showed that Gremlin1 promotes the activation of HSCs and subsequent hepatic fibrosis by enhancing TGF-β signaling and suppressing BMP signaling.[7] In addition, Gremlin1, DAN family BMP antagonist, a potential target of the miR-23b/27b/24-1 cluster, has been reported previously to inhibit TGF-β signaling in the embryonic development of the liver.[21] Therefore, we investigated the role of the miR-23b/27b/24-1 cluster in HSC activation and hepatic fibrosis. In this report, we show that the miR-23b/27b/24-1 cluster inhibited hepatic fibrogenesis by directly targeting mRNAs and down-regulated 5 secretive hepatic fibrosis–related proteins important in HSC activation and increased ECM protein secretion or deposition. Finally, we explored TGF-β– and integrin-mediated signaling pathways involving the miR-23b/27b/24-1 cluster and hepatic fibrosis–related proteins.

Results

The miR-23b/27b/24-1 Cluster Ameliorates Mouse Hepatic Fibrosis in Vivo

The miR-23b/27b/24-1 cluster is highly conserved across vertebrates (Figure 1*A*) and belongs to the heterosequence seed cluster (Figure 1*B*). To determine whether the exogenous miR-23b/27b/24-1 cluster differentially and sequentially expresses each member of the cluster as an endogenous cluster, real-time polymerase chain reaction (PCR) was performed after the pCDH-miR-23b/27b/24-1 plasmid was transfected into HSC-T6 cells, and the results verified that the exogenous miR-23b/27b/24-1 cluster effectively expresses miR-23b-5p/3p, miR-27b-5p/3p, and miR-24-1-5p/3p, as expected (Figure 1*C* and *D*). After CCl_4-induced mouse hepatic fibrosis models were established and lentivirus therapy was administered, a biopsy of the liver was performed, and the resulting samples showed an obvious gross nodular pattern in the CCl_4-treated and analogue (LV-Puro) groups. In addition, the appearance of the liver was completely benign, with neither nodules nor fibrotic septa in the mice that received LV-miR-23b/27b/24-1 (Figure 1*E*). Liver histology (H&E staining) of the CCl_4-treated and LV-Puro group samples showed abundant bridging necrosis and established pseudonodules of uneven sizes in a background of diffuse cellular swelling and relatively mild inflammatory cell infiltration. Correspondingly, LV-miR-23b/27b/24-1 significantly prevented bridging necrosis and destruction of the liver architecture, as well as cellular swelling. Two-photon excited fluorescence/second harmonic generation (TPEF/SHG) imaging with a dual-

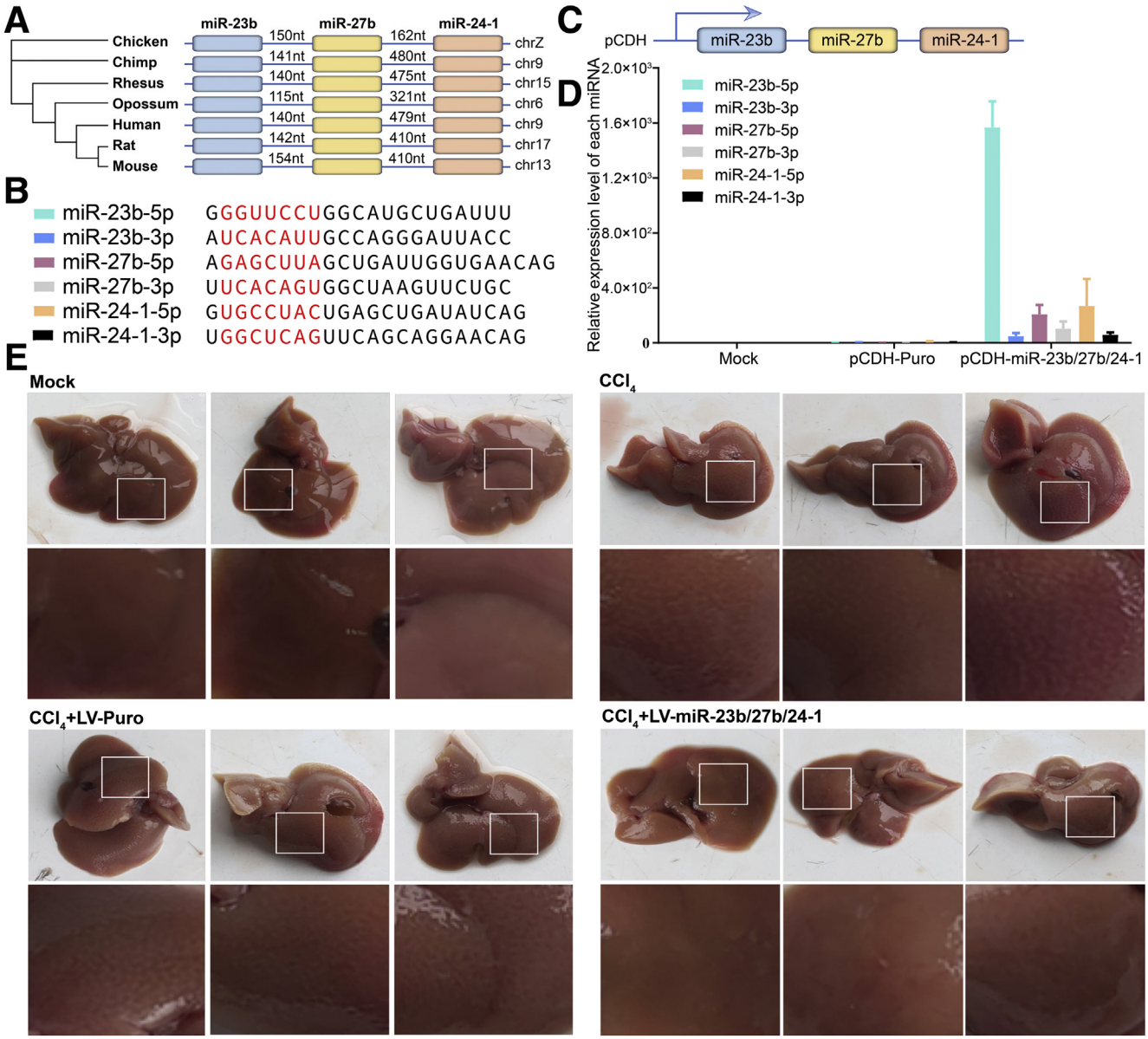

Figure 1. The miR-23b/27b/24-1 cluster significantly alleviated CCl_4-induced mouse hepatic fibrosis, as indicated by gross appearance of the liver (n = 3 per group). (*A*) The evolution of the miR-23b/27b/24-1 cluster in animals. (*B*) The mature sequence of miRNAs in the miR-23b/27b/24-1 cluster. The seed regions (positions 2–8) are labeled in red. (*C*) The gene structure of the pCDH-miR-23b/27b/24-1 plasmid. (*D*) Real-time PCR analysis of individual miRNAs after HSC-T6 cells were transfected with pCDH-miR-23b/27b/24-1. Levels of specific individual mRNAs are reported relative to that of U6. The relative intensity of each miRNA was determined relative to that of the control, which was set to 1. (*E*) Mice received saline (Mock and CCl_4 groups), an inactive analogue (LV-PURO+CCl_4 group), or miR-23b/27b/24-1 (LV-miR-23b/27b/24-1+CCl_4 group) (n = 3). A view of a complete liver is shown in each quadrant of the *upper panels*, and a close-up view of a liver is shown in each quadrant of the *lower panels*.

photon microscope showed sensitive and specific detection of fibrous collagen disposition (green) in the hepatic parenchyma (red).[22] The investigation performed by classic Masson's trichrome blue staining for collagen and TPEF/SHG imaging showed marked attenuation in collagen deposition in the mice that received miR-23b/27b/24-1 compared with the control (Figures 2*A* and 3). Histologic scoring of fibrosis and neuroinflammatory activity also were performed in a blinded fashion, and the scores of the LV-miR-23b/27b/24-1 group were obviously lower than those of the CCl_4-treated and LV-Puro groups (Table 1).

Subsequently, an algorithm was used to systematically quantitate collagen deposition on the basis of image analysis,[23] and the TPEF/SHG data showed a significant reduction in the total collagen percentage, aggregated collagen percentage, distributed collagen percentage, number of long strings, string area, string length, string width, string perimeter, and number of crosslinks (Figure 2*B*).

The miR-23b/27b/24-1 Cluster Suppresses TGF-β1–induced Profibrotic Genes

To explain how the miR-23b/27b/24-1 cluster influences HSCs, fresh primary rat HSCs were isolated and activated by the TGF-β1 protein. Then, HSCs were infected with LV-miR-23b/27b/24-1, and RNA sequencing (RNA-seq) was performed to analyze the changes in mRNA expression of all genes. The results of a comparison of the group treated with both LV-miR-23b/27b/24-1 and TGF-β1 and that treated with LV-puro and TGF-β1 showed that differences in the mRNA expression of 71 genes central to hepatic fibrogenesis were mediated by the miR-23b/27b/24-1 cluster (Figure 4*A*). The proteins encoded by these genes included 18 TGF superfamily members, 22 ECM proteins, 16 ITGs, 4 LOXs, 3 TIMPs, and 8 MMPs. In addition, the mRNAs of 60 proteins that promote HF (16 TGF-β proteins, 21 ECM proteins, 16 ITGs, 4 LOXs, and 3 TIMPs) were down-regulated, except for Vitronectin and ITGβ7. Only the mRNA expression of 7 antifibrosis-related proteins (6 MMPs and BMP6) was down-regulated; however, that of MMP3 and MMP13 was up-regulated (Figure 4*B*).

Identification of miR-23b/27b/24-1 Cluster Targets Using the Predictor-WJF Algorithm and RNA-Seq

The aforementioned findings show the attenuating effect of the miR-23b/27b/24-1 cluster on hepatic fibrosis in vivo and HSCs in vitro, but the particular mechanism needed to be explored further. Computational algorithms are widely used to identify targets of certain miRNAs; however, false positives are difficult to avoid. To identify the targets of miRNA(s), the Predictor-WJF algorithm was developed. A flowchart showing the steps of the Predictor-WJF is presented in Figure 4*C*. The targets of the miR-23b/27b/24-1 cluster were identified in 2 steps using the Predictor-WJF algorithm and performing RNA-seq. In the first step, a total of 171 hepatic fibrosis–related genes in 6 categories were manually selected as candidate genes. Each candidate gene predicted to be a target of miR-23b, miR-27b, and miR-24-1 in at least 1 of the 6 data sets of Predictor-WJF was given a score; 1 point was added to the score of a gene for every computational prediction algorithm in which it was identified, and 2 points were added to the score of genes in the The Encyclopedia of RNA Interactomes (ENCORI) database, in which data undergo experimental validation. The final score for a candidate gene of a miRNA is the sum of the points corresponding to the identification of the gene in a data set; the maximum score is 7, and score of a example gene named "D" is 5 (Figure 4*C*). Potential targets of each miRNA in the miR-23b/27b/24-1 cluster with a score higher than or equal to 5 were extracted.

In the second step, potential targets were filtered on the basis of RNA-seq data, and those with considerable basic expression levels and that showed substantial changes after stimulation with anaplastic lymphoma kinase 5 (ALK5) or miRNA treatment (with log[fold change]>1.5 and $P < .001$) ultimately were identified as targets. In total, 3 targets of miR-23b (the mRNAs of *Gremlin1*, *Tgfbr2*, and *Col4a1*) and 5

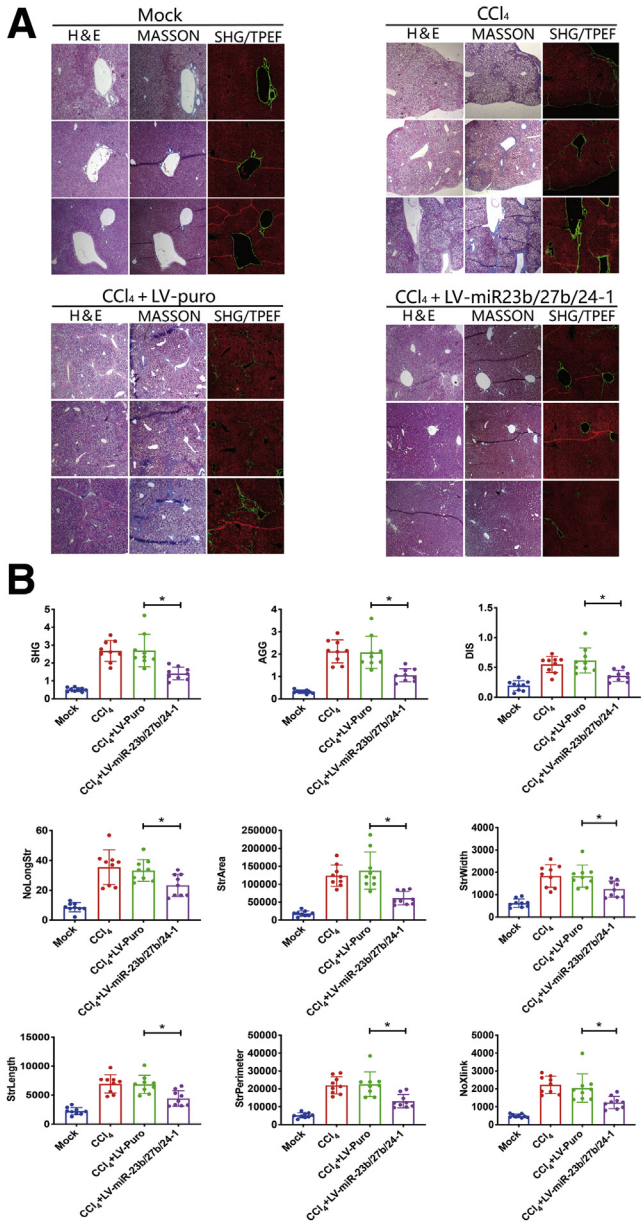

Figure 2. The miR-23b/27b/24-1 cluster reduced hepatic collagen deposition in CCl_4-induced mouse hepatic fibrosis, as determined by H&E staining, Masson's trichrome blue staining, and TPEF/SHG (n = 3 per group). (*A*) Serial sections of 3 distinct samples of each of the 12 livers were obtained. Histopathology of serial slices was performed with H&E staining and Masson's trichrome blue staining for collagen following standard procedures, and the serial sections were delivered to Hangzhou Chou-Tu Technology Company for TPEF/SHG analysis. (*B*) miR-23b/27b/24-1 alleviated collagen deposition and 8 other related parameters. Nine parameters associated with collagen deposition were analyzed by TPEF/SHG: SHG, second harmonic generation, indicates total collagen percentage of area; Agg, aggregated collagen percentage; Dis, distributed collagen percentage; NoLongStr, number of long strings; StrArea, string area; StrLength, string length; StrWidth, string width; StrPerimeter, string perimeter; and NoXlink, number of crosslinks. Statistical significance was calculated by 1-way analysis of variance. *$P < .05$.

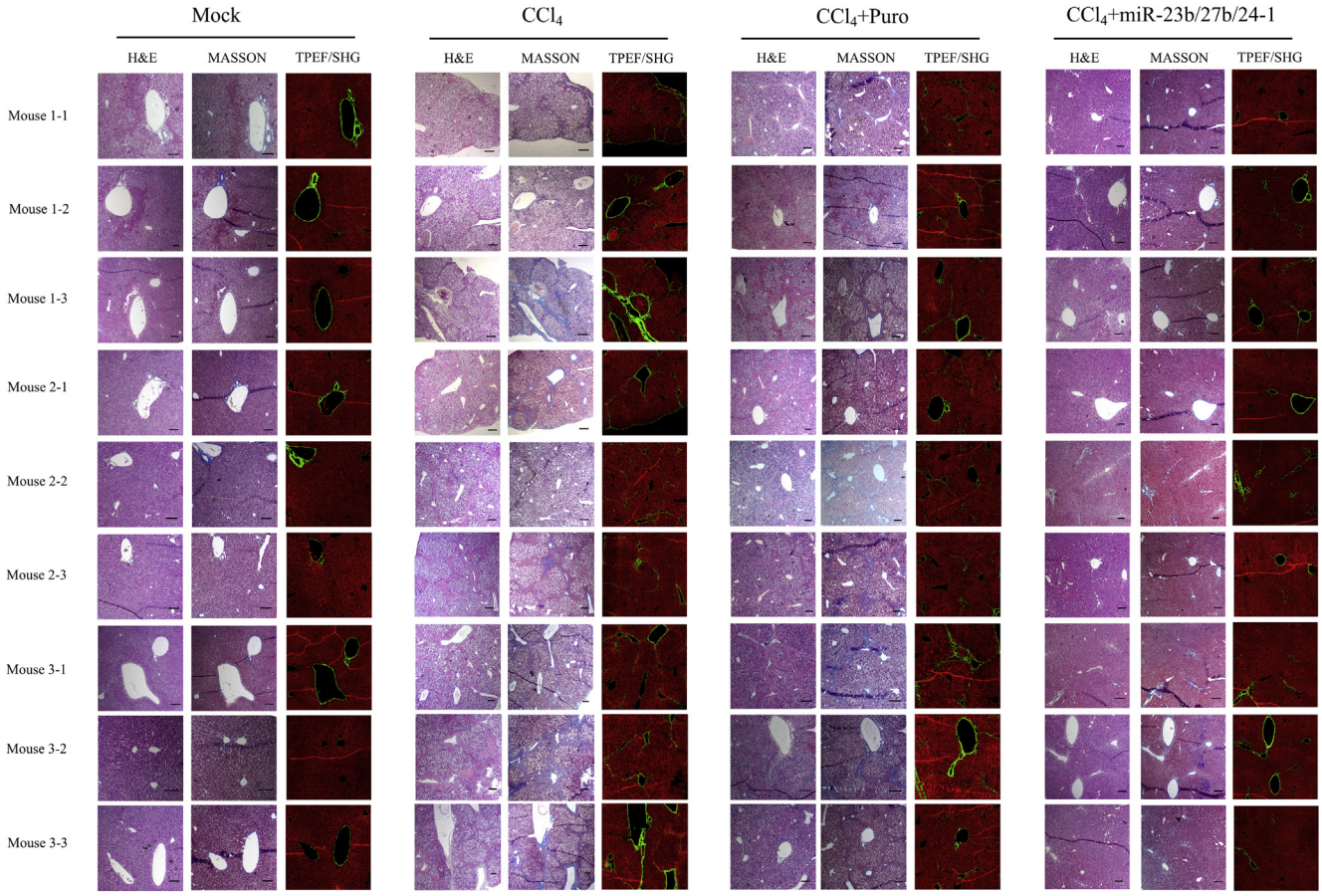

Figure 3. miR-23b/27b/24-1 cluster reduced hepatic collagen deposition in CCl^4-induced mouse hepatic fibrosis by H&E staining, Masson's trichrome blue staining and TPEF/SHG. Serial sections of 3 discontinued parts in each of 12 livers were obtained. Histopathology by H&E staining and Masson's trichrome blue staining for collagen of serial slices were performed as the following standard procedure and the serial sections were delivered to the Hangzhou Chou-Tu Technology Company for TPEF/SHG analysis. Representative photographs of H&E staining, Masson's staining, and TPEF/SHG of each of 3 discontinued parts in the 12 livers are shown here.

targets of miR-27b (the mRNAs of *Gremlin1*, *Itga5*, *Itga2*, *Lox*, and *Tgfr1*) were identified. Considering that proliferative and fibrogenic growth factors such as TGF-β and connective tissue growth factor (CTGF) play pivotal roles in the activation of HSCs and hepatic fibrosis,[24] and that *Tgfb2* ranked first among all growth factor genes (the *Tgfb2* score with respect to miR-23b = 4) and was verified by RNA-seq, Tgfb2 mRNA also was considered a target of miR-23b and worthy of further investigation. Notably, the prediction of the miR-24-1 targets obtained through the Predictor-WJF algorithm was not as efficient as that of the other 2 miRNAs in the cluster owing to the lack of experimentally validated data; thus, the top 2 candidate genes of miR-24-1 with RNA-seq verification (*Mmp14* and *Lox*) were considered valuable for further investigation. In addition, *Mmp14* ranked first among all the Mmp family genes targeted by mir-24-1. To date, 4 targets of miR-23b (the mRNAs of *Gremlin1*, *Tgfbr2*, *Col4a1*, and *Ttfb2*), 5 targets of miR-27b (the mRNAs of *Gremlin1*, *Itga5*, *Itga2*, *Lox*, and *Tgfbr1*), and 2 targets of miR-24-1 (the mRNAs of *Mmp14* and *Lox*) have been identified (Figure 4*D*).

The miR-23b/27b/24-1 Cluster Directly Targets the mRNAs of 5 Profibrotic Genes

To further explore whether the miR-23b/27b/24-1 cluster directly targets mRNAs of profibrotic genes, a luciferase reporter assay was performed. The results showed that among the 10 conserved potential targets, the luciferase activity of the *Tgfb2*, *Gremlin1*, *Lox*, *Itga2*, and *Itga5* reporter plasmids was remarkably decreased after co-transfection with miRNA mimics, while the luciferase activity of the other 5 target genes changed negligibly. Moreover, the down-regulated luciferase activity was completely inhibited once the miRNA binding sites on the 3′ untranslated region (UTR) of the target genes were mutated. The interferences of endogenous miR-23b or other endogenous miRNAs (eg, *Tgfb2* is predicted to be a target of miR-200a and miR-141, *Itga2* is predicted to be a target of miR-30, and *Itga2* is predicted to be a target of miR-26 by the TargetScan database), help to explain some unexpected findings, such as the luciferase levels were much lower when they added on the 3'UTR of *Tgfb2*/*Itga2*/*Itga5* compared with the pMIR-Luc (pMIR-REPORT™ Luciferase; RiboBio Co, Guangzhou, China) vector controls. To further

Table 1. Histologic Scoring of 12 Individual Livers (Scheuer 1991)[50]

Number	Fibrosis	Necroinflammatory activity
Mock 1	0	0
Mock 2	0	0
Mock 3	0	0
CCl_4 1	3	4
CCl_4 2	3	4
CCl_4 3	3	4
CCl_4+Lv-puro 1	3	4
CCl_4+Lv-puro 2	3	4
CCl_4+Lv-puro 3	3	4
CCl_4+Lv-miR23b/27b/24-1 1	0	0
CCl_4+Lv-miR23b/27b/24-1 2	0	0
CCl_4+Lv-miR23b/27b/24-1 3	0	0

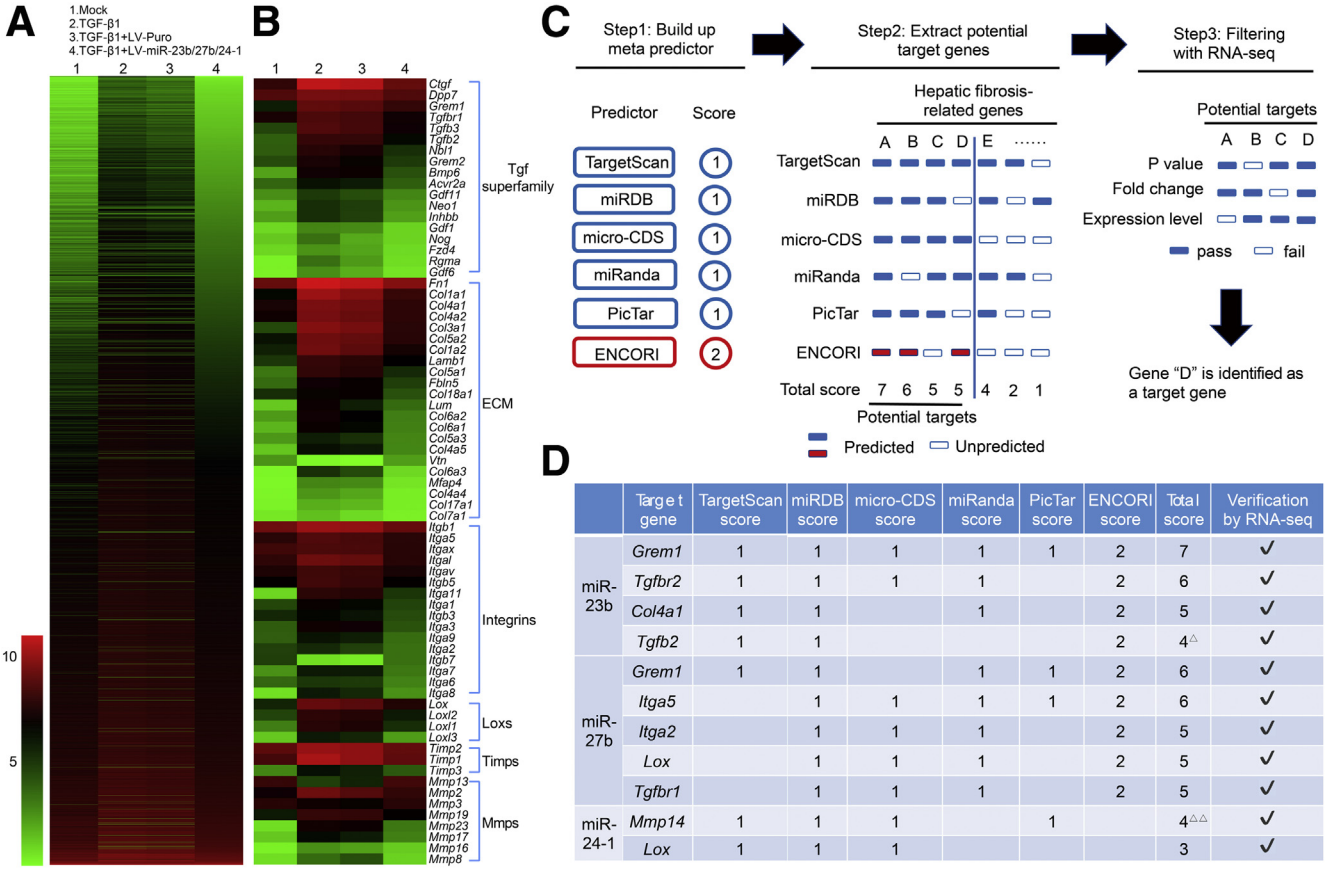

	Target gene	TargetScan score	miRDB score	micro-CDS score	miRanda score	PicTar score	ENCORI score	Total score	Verification by RNA-seq
miR-23b	*Grem1*	1	1	1	1	1	2	7	✓
	Tgfbr2	1	1	1	1		2	6	✓
	Col4a1	1	1		1		2	5	✓
	Tgfb2	1	1				2	4△	✓
miR-27b	*Grem1*	1	1		1	1	2	6	✓
	Itga5		1	1	1	1	2	6	✓
	Itga2		1	1	1		2	5	✓
	Lox		1	1	1		2	5	✓
	Tgfbr1		1	1	1		2	5	✓
miR-24-1	*Mmp14*	1	1	1		1		4△△	✓
	Lox	1	1	1				3	✓

Figure 4. Identification of gene targets of the miR-23b/27b/24-1 cluster as determined by use of the Predictor-WJF algorithm and RNA-seq. (*A* and *B*) Heatmap comparing 4899 differentially expressed genes and 71 hepatic fibrosis–related genes between the LV-miR-23b/27b/24-1 and LV-Puro groups of rat primary HSCs. Euclidean clustering of both *rows* and *columns* using $\log_2$-RNA-seq expression data; n= 3 per group. (*C*) Flowchart showing the Predictor-WJF algorithm used to identify gene targets of the miR-23b/27b/24-1 cluster. Predictor-WJF incorporates 5 independent computational target prediction algorithms and 1 data set of experimentally validated miRNA targets. Each gene predicted as a target of a miRNA in any 1 of the 6 data sets was assigned a score. The points awarded for inclusion in the data sets were added to produce a final score for each potential target gene, and the rank order of the genes was determined. Then, the RNA-seq results were used to filter the target genes further. Potential target genes that were differentially expressed between the LV-miR-23b/27b/24-1 and LV-Puro groups of rat primary HSCs were recognized as target genes in this study. *Differentially expressed* refers to gene expression differences with a *P* value $< .05$ (DEseq2), a |fold change| >2, and fragments per kilobase of transcript per million mapped reads (FPKM) >1 in each group. (*D*) Target genes of the miR-23b/27b/24-1 cluster identified by Predictor-WJF and RNA-seq.

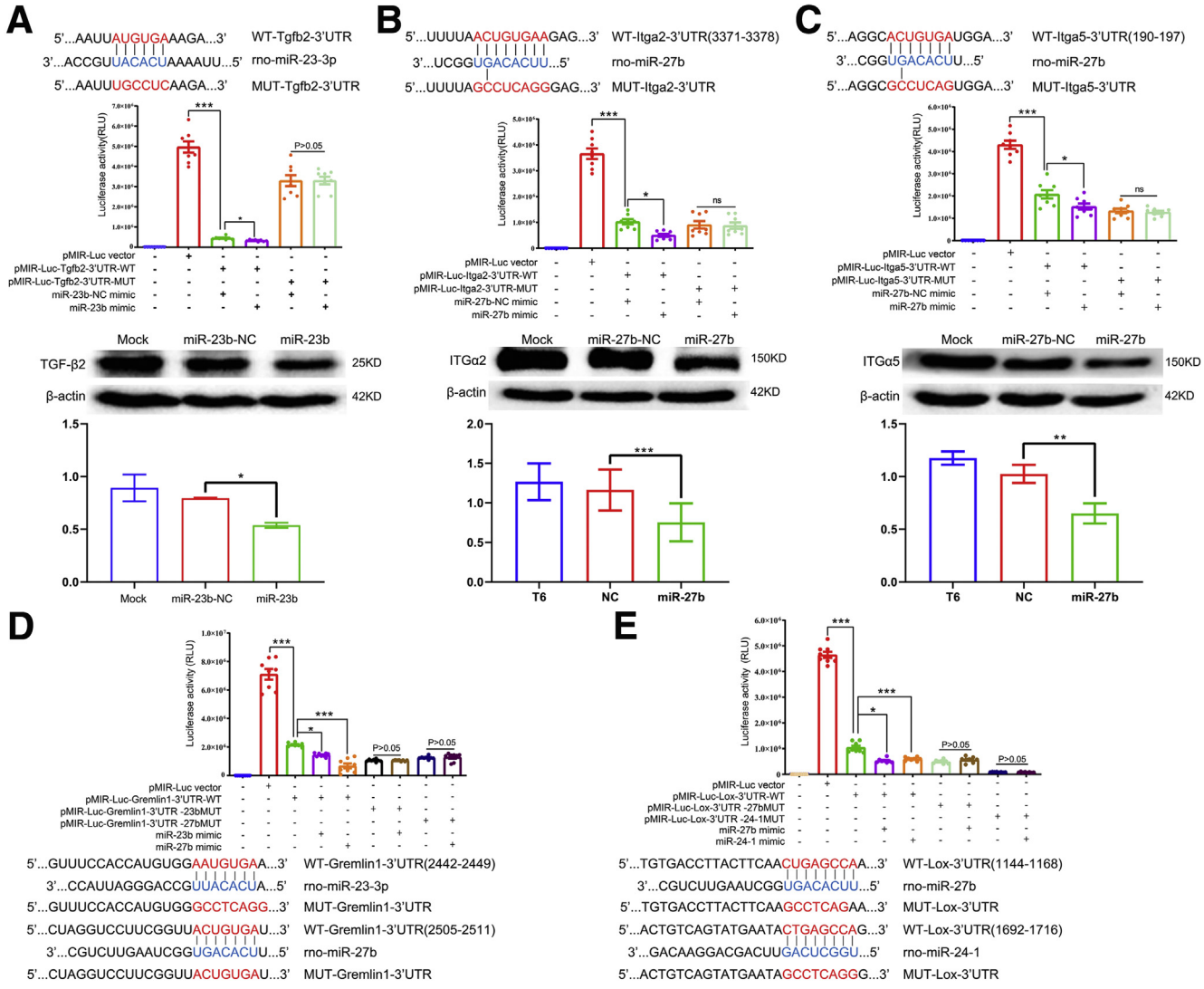

Figure 5. The miR-23b/27b/24-1 cluster directly targets mRNAs of 5 profibrotic genes. (*A*) The core miR-23b binding site and the mutated sites in the 3′ UTR of rat *TGF-β2*. Luciferase assay was performed to verify the direct regulatory effect of miR-23b on TGF-β2 expression. The protein level of TGF-β2 was analyzed by Western blot after HSC-T6 cells were transfected with the miR-23b mimics (n = 3 per group). (*B* and *C*) The core miRNA-27b binding sites and the mutated sites in the 3'UTR of rat *ITGα2/5*. Luciferase assay was performed to verify the direct regulatory effect of miRNA-27b on ITGα2/5 expression. The protein level of ITGα2/5 was analyzed by Western blot after HSC-T6 cells were transfected with the miRNA-27b mimics (n = 3 per group). (*D*) Core miR-23b, miR-27b binding site and mutated sites in the 3'UTR of rat *Gremlin1*. Luciferase assay was performed to verify the direct regulatory effect of miR-23b and miR-27b on Gremlin1 expression (n = 3 per group). (*E*) Core miR-27b, miR-24-1 binding site and mutated in the 3'UTR of rat *LOX*. Luciferase assay was performed to verify the direct regulatory effect of miR-27b and miRNA-24-1 on LOX expression (n = 3 per group). **P* < .05, ***P* < .01, ****P* < .001. RLU, relative light unit.

evaluate the effects of the miRNAs on the protein expression levels of the 5 target genes, Western blot analysis were performed, and we found that the protein expression of these genes was inhibited following the same pattern of luciferase activity inhibition; that is, miR-23b directly targeted the mRNA of *TGF-β2*, miR-27b directly targeted the mRNAs of *Itgα2* and *Itgα5*, miR-23b and miR-27b directly and simultaneously targeted the mRNA of *Gremlin1*, and miR-27b and miR-24-1 directly and synergistically targeted the mRNA of *LOX* (Figures 5 and 6).

Bioinformatic Analyses of Differentially Expressed Hepatic Fibrosis–Related Genes Regulated by the miR-23b/27b/24-1 Cluster

Gene Ontology (GO), Kyoto Encyclopedia Genes and Genomes (KEGG), protein–protein interaction, and GeneMANIA analyses were performed to predict the functions and molecular interactions of the 71 differentially expressed hepatic fibrosis–related genes regulated by the miR-23b/27b/24-1 cluster in HSCs. The GO analysis indicated that the encoded proteins were localized mainly outside the cell,

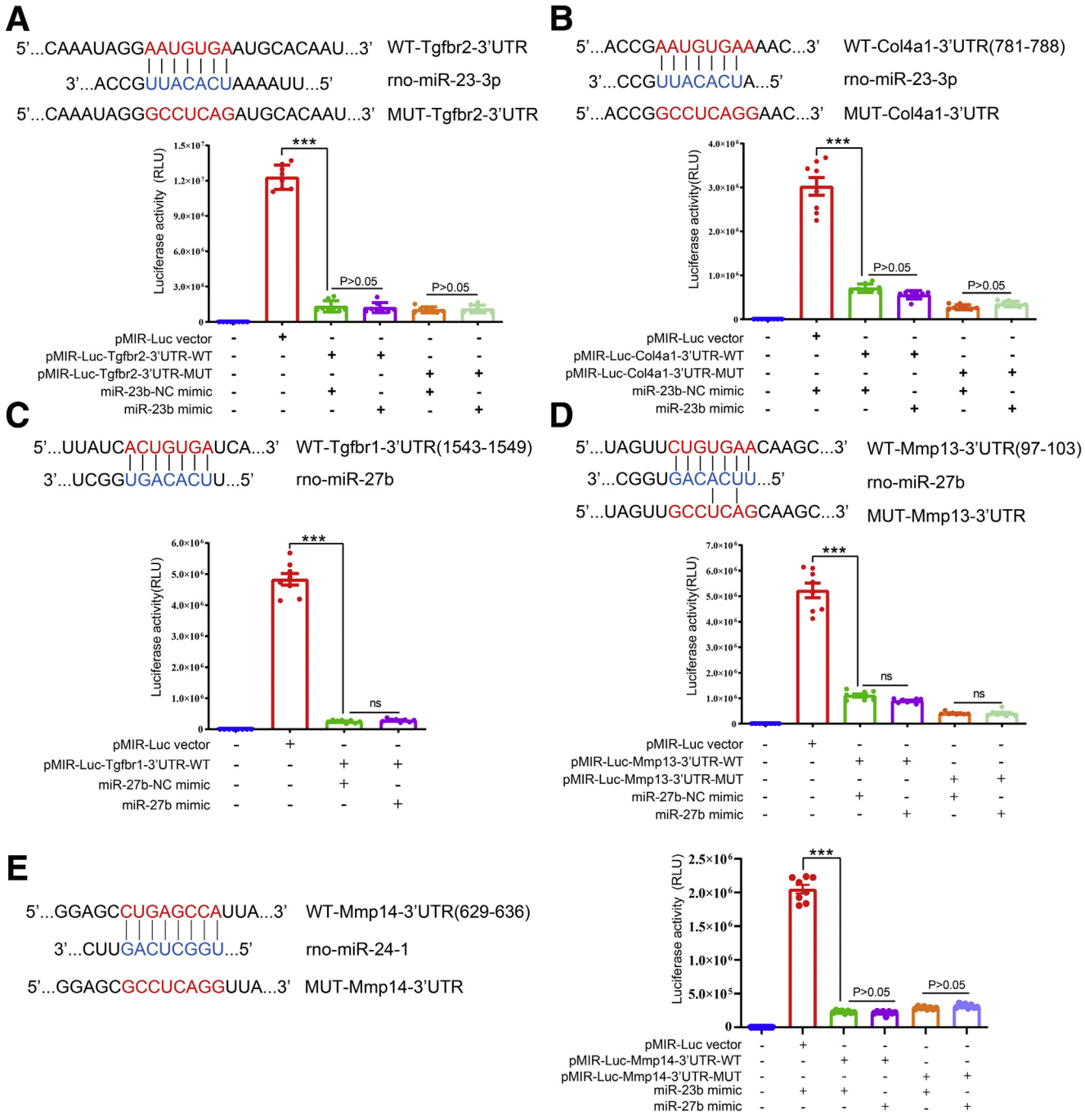

Figure 6. The regulations of miR-23b/27b/24-1 cluster on TGF-βr1/2, MMP13/14, and COL4α1. (*A* and *B*) The core miR-23b binding sites and the mutants on the 3'UTR of rat *TGF-βr2* or *COL4α1*; Luciferase assays to verify the direct regulation effect of miR-23b on *TGF-βr2* or *COL4α1*. (*C* and *D*) The core miRNA-27b binding sites on the 3'UTR of rat *TGF-βr1* or *MMP13*; Luciferase assays to verify the direct regulation effect of miRNA-27b on *TGF-βr1* or *MMP13*. (*E*) The core miR-24-1 binding site and the mutant on the 3'UTR of rat *MMP14*. Luciferase assay to verify the direct regulation effect of miR-24-1 on *MMP14*. All results are expressed as means ± SD. ***$P < .001$.

such as in the extracellular space, extracellular exosomes, at the cell surface, and in the extracellular region. These proteins were found to be in the ECM, proteinaceous ECM, basement membrane, collagen trimers, and integrin complexes (Figure 7*A*). These proteins primarily were involved in the integrin-mediated signaling pathway, cell and cell-matrix adhesion, collagen fibril organization, and the positive regulation of pathways inhibiting SMAD protein phosphorylation (Figure 7*B*), and they also were associated with receptor binding, such as integrin binding, collagen binding, TGF-β–receptor binding, fibronectin binding, and laminin binding (Figure 7*C*).

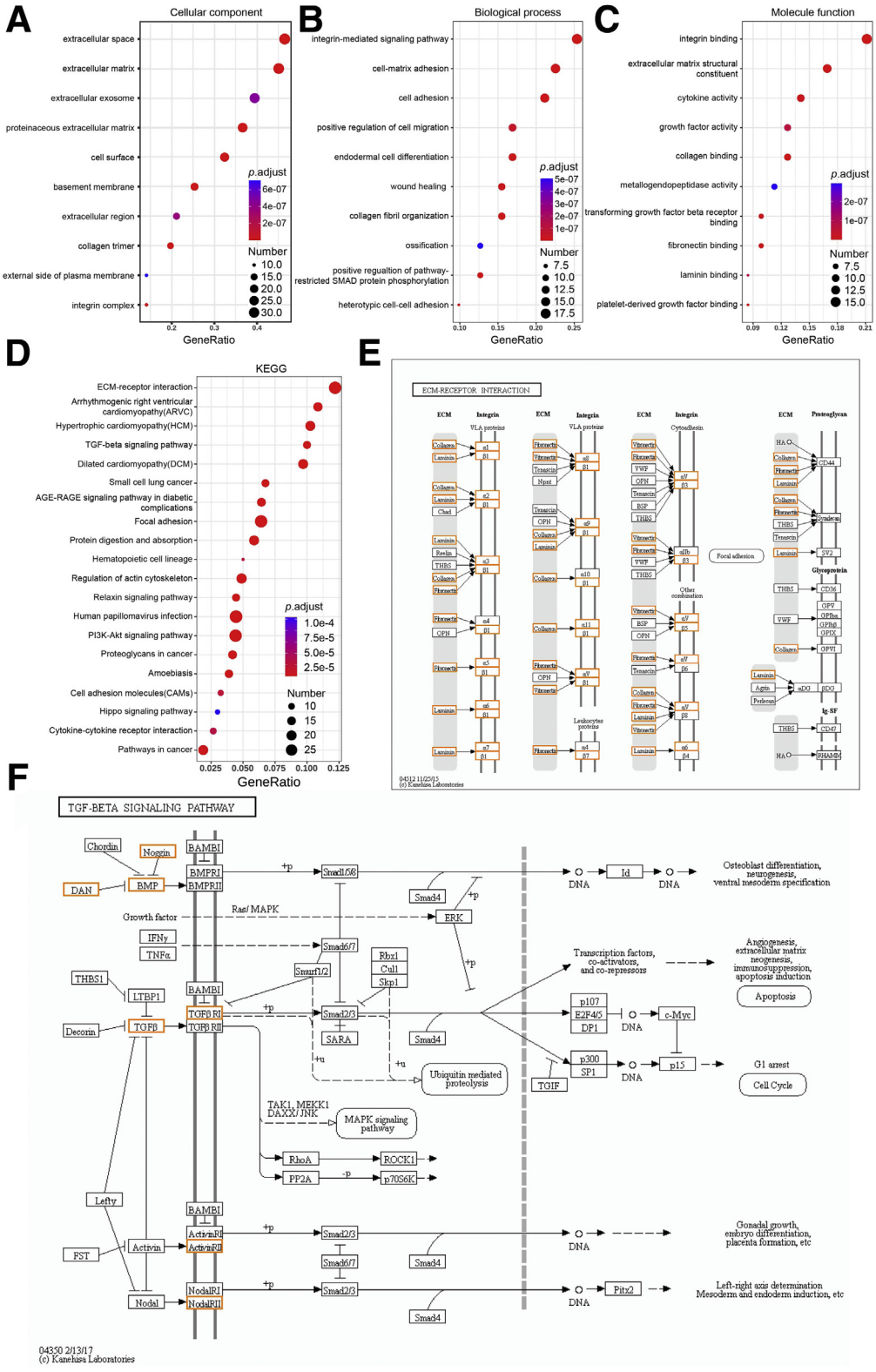

Figure 7. GO annotations and KEGG analyses of the differentially expressed hepatic fibrosis–related genes regulated by the miR-23b/27b/24-1 cluster in primary rat HSCs. (*A–C*) The graphs present the degree of enrichment of the significantly enriched genes associated with GO terms in the biological process, cellular component, and molecular function categories. (*D*) Graphic showing KEGG analysis. The enrichment ratio (the ratio of the number of genes in an annotated set that are selected on the basis of a specific number of target genes to the total number of genes annotated; the enrichment ratio = term candidate gene number/term gene number) represents the degree of enrichment of differentially expressed genes. The y-axis shows the name of enriched pathways. The area of each node represents the number of enriched differentially expressed

The KEGG analysis showed that the 71 differentially expressed hepatic fibrosis–related proteins were associated mainly with ECM-receptor interactions, TGF-β signaling pathways, and focal adhesion (Figure 7*D*). These proteins mapped to 79 KEGG pathways; notably, most of these proteins were involved in 2 important fibrosis-related pathways: the ECM-receptor interaction axis and the TGF-β signaling pathway. Collagens and integrins play important roles in ECM-receptor interactions. Gremlin1 and TGF-β proteins also play important roles in the TGF-β signaling pathway (Figure 7*E* and *F*).

In the protein–protein interaction (PPI) network construction and module analysis, the first 3 of 4 modules were associated by gene number and score. In module 1, both ITGα2 and ITGα5 interacted with 8 proteins, including COLIα1, COLIα2, COLVIα1, COLVIα2, FN1, ITGβ1, ITGβ7, and LAMβ1. ITGα2 also interacted with LUMICAN. In module 3, both LOX and TGF-β2 interacted with CTGF, MMP13, and TIMP1. TGF-β2 also interacted with TGF-β receptor 1 (TGF-βR1), and LOX also interacted with MMP3 and TIMP2 (Figure 8*A*).

Using GeneMANIA to construct a PPI network, we found that in a network comprising 147 genes in the genome, the protein products of 10 genes responded to TGF-β; in a network of 115 genes in the genome, the protein products of 11 genes were in the BMP signaling pathway, and in a network of 46 genes in the genome, the protein products of 9 genes were involved in the integrin-mediated signaling pathway. We further investigated the colocalization and co-expression of the protein products of the 5 target genes of the miR-23b/27b/24-1 cluster as well as the related proteins. The network analysis showed that LOX was colocalized and co-expressed with 13 proteins. Gremlin1, TGF-β2, ITGα2, and ITGα5 were co-expressed with 16, 7, 10, and 6 proteins, respectively (Figure 8*C*).

The miR-23b/27b/24-1 Cluster Effectively Down-Regulated the Expression of Hepatic Fibrosis–Related Proteins in HSCs

We clarified that each member of the miR-23b/27b/24-1 cluster directly down-regulates the expression of 5 target genes, but whether the cluster plays a biological role as a whole in HSC-T6 cells and primary HSCs remains to be determined on the basis of more data. After transfection with the pcDNA3.1-CA-ALK5 plasmid for 24 hours, HSC-T6 cells were transfected with the pCDH-miR-23b/27b/24-1 plasmid to explore the down-regulating role of the cluster on hepatic fibrosis genes, and Western blot analysis showed that ALK5 observably up-regulated the protein expression levels of TGF-β2, Gremlin1, LOX, ITGα2, ITGα5, COLIα1, COLIα2, TGF-β1, and TIMP1; however, the up-regulating effect of ALK5 was inhibited dramatically by the miR-23b/27b/24-1 cluster, while the expression of MMP9 changed negligibly (Figure 9*A–D*). To verify the reliability of the findings showing the miR-23b/27b/24-1 cluster acting on HSCs, fresh primary rat HSCs were isolated and stimulated to activate TGF-β1 protein. Then, the HSCs were infected with LV-miR-23b/27b/24-1, and Western blot analysis showed that TGF-β1 observably up-regulated the protein expression levels of LOX and COLIα1; however, the up-regulating effect of TGF-β1 was inhibited dramatically by the miR-23b/27b/24-1 cluster (Figure 9*E* and *F*).

Discussion

Because numerous hepatic fibrosis agonists and antagonists participate in HSC activation and hepatic fibrosis, it is difficult to treat hepatic fibrosis in clinical practice.[4,16] To activate HSCs, scientists have explored target delivery tools, but thus far, no ideal tool has been applied successfully in practice.[25,26] To create a multitarget antifibrotic regimen to simultaneously suppress multiple hepatic fibrosis agonists and/or enhance multiple hepatic fibrosis antagonists, we overexpressed miR-23b/27b/24-1 through intravenous delivery of miR-23b/27b/24-1 lentivirus. In 2009, Rogler et al[21] published a report in *Hepatology* suggesting that the miR-23b/27b/24-1 cluster targets and down-regulates Smad2, 3, and 4, inhibiting TGF-β signaling. In 2017, these investigators provided evidence to support this idea.[27] Although activated TGF-β signaling promotes hepatic fibrosis, they reported here that knockdown of miR-23, miR-27, and miR-24 blocked hepatic fibrosis by antagomir-23b-3p, antagomir-27b-3p, and antagomir-24-1-3p in mice. Our data establish that miR-23b/27b/24-1 cluster overexpression suppressed HSC activation by directly targeting mRNAs, reducing the protein expression of TGF-β2, Gremlin1, LOX, ITGα2, and ITGα5. In addition, the overexpressed miR-23b/27b/24-1 cluster decreased ECM protein secretion and increased ECM degradation through suppression of TGF-β signaling. In summary, the miR-23b/27b/24-1 cluster blocked hepatic fibrosis in mice.

Hepatic fibrosis is characterized by ECM deposition, which contributes to cirrhosis.[1] Unfortunately, ECM deposition has not been attenuated effectively. HSC activation and transdifferentiation are central drivers of hepatic fibrosis. Enhancement of hepatic fibrosis agonists and/or suppression of hepatic fibrosis antagonists lead to HSC activation, resulting in increased ECM protein secretion and decreased ECM degradation.[24] However, the heterosequence seed cluster of miR-23b/27b/24-1 potentially targets mRNAs of many hepatic fibrosis–related proteins that influence ECM deposition. Our study provides

hepatic fibrosis–related genes regulated by the miR-23b/27b/24-1 cluster. The *P* value is represented by a color scale. The statistical significance increases from blue (relatively low significance) to orange (relatively high significance). (*E*) Specific interactions between cells and the ECM are mediated by integrins. (*F*) Differentially expressed hepatic fibrosis–related proteins participate in the TGF-β and BMP signaling pathways. The differentially expressed genes obtained through high-throughput RNA-seq and enriched in the pathway are highlighted by *yellow boxes*. PI3K-Akt, Phosphatidylinositol 3-kinase/serine-threonine protein kinase.

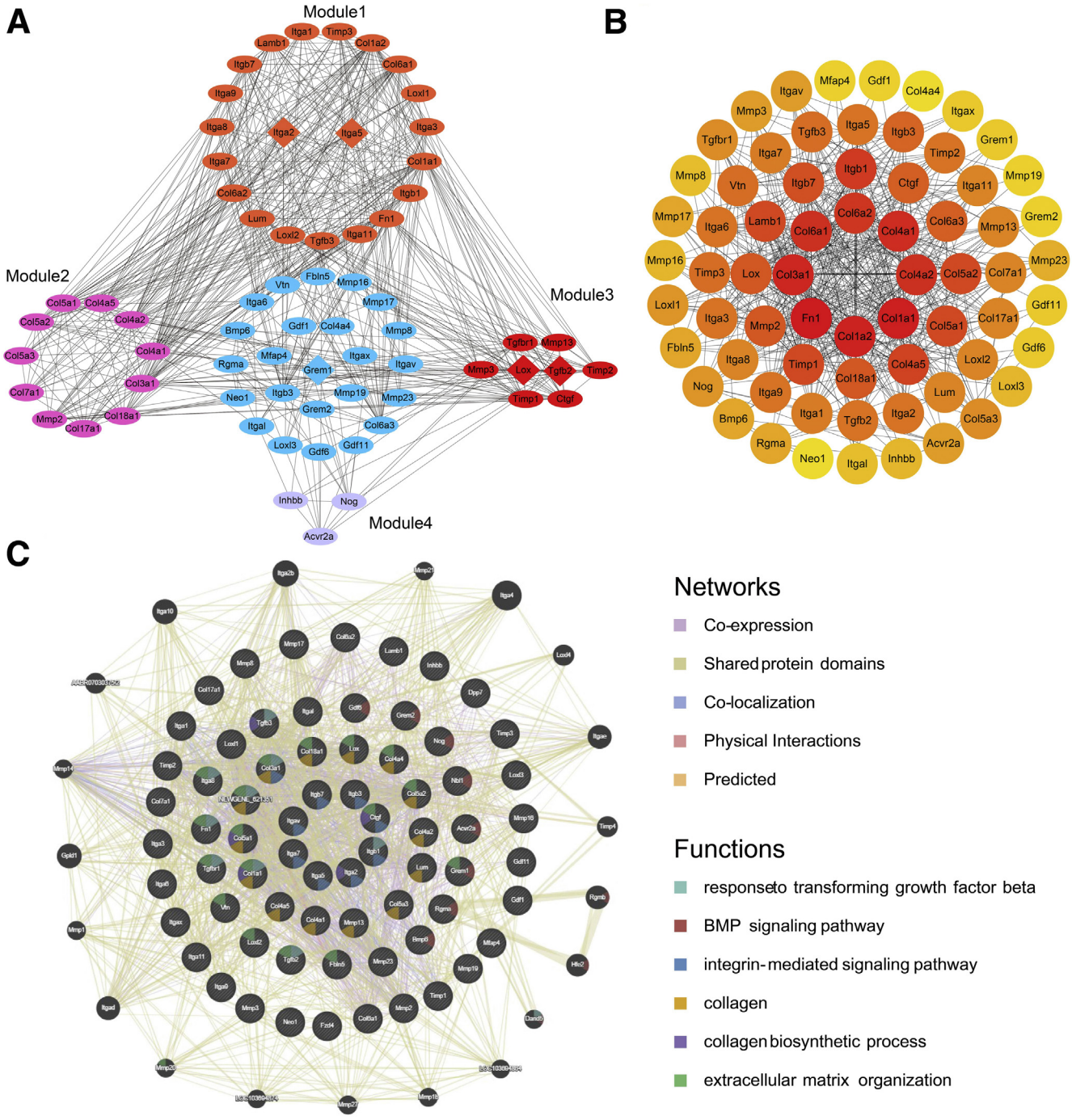

Figure 8. PPI network construction and analysis of the differentially expressed hepatic fibrosis–related genes regulated by the miR-23b/27b/24-1 cluster in primary rat HSCs. (*A*) PPI network construction and module analysis. The *light blue nodes* in the middle represent the differentially expressed genes identified. The surrounding *colored nodes* represent the genes involved in 4 modules, and the *lines* represent the interaction between 2 nodes. The score of module 1 is 11.5, the score of module 2 is 10.2, the score of module 3 is 5.429, and the score of module 4 is 3. Five target genes regulated by the miR-23b/27b/24-1 cluster, *Itga2*, *Itga5*, *Lox*, *Tgfb2,* and *Grem 2*, are in the center of the *circles*. (*B*) PPI network analysis. All genes were chosen using the degree method and the CytoHubba plugin, and the higher ranking is represented by a more intense red. (*C*) Network and functional analysis (GeneMANIA) showing the gene set that was enriched in the network. The different colors of the network edges indicate the bioinformatics analysis applied: website prediction, co-expression, shared protein domains, physical interactions, and colocalization. The different colors of the network nodes show the biological functions of the enriched genes. NEWGENE_621351 is Col1a2.

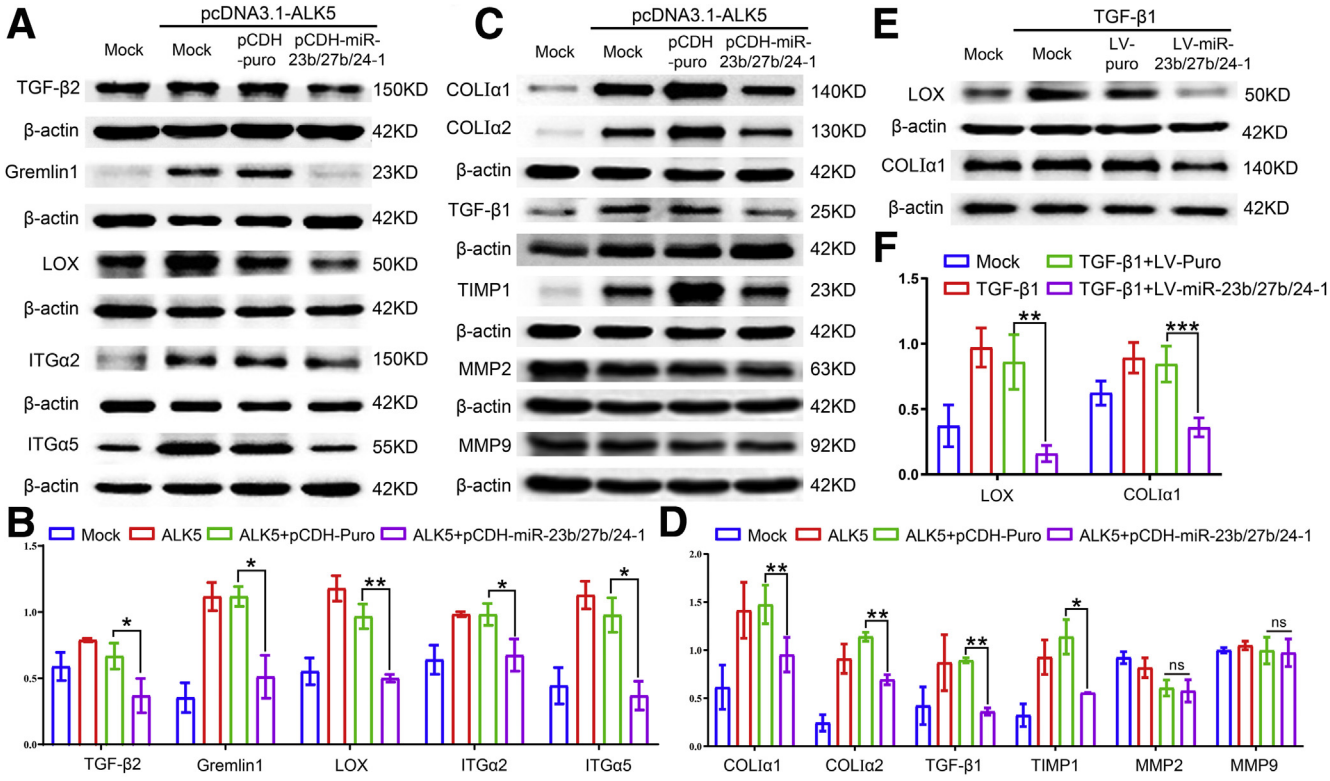

Figure 9. The miR-23b/27b/24-1 cluster effectively inhibited the expression of hepatic fibrosis–related genes. (*A* and *B*) Western blots showing that the miR-23b/27b/24-1 cluster down-regulated the expression of 5 target genes in HSC-T6 cells, including *TGF-β2*, *Gremlin1*, *LOX*, *ITGα2*, and *ITGα5*. (*C* and *D*) Western blots showing that the miR-23b/27b/24-1 cluster regulated the expression of 5 hepatic fibrosis–related genes in HSC-T6 cells, including *COLIα1*, *COLIα2*, *TGF-β1*, and *TIMP1*. (*E* and *F*) Western blots showing that the miR-23b/27b/24-1 cluster down-regulated the expression of LOX and COLIα1 in primary rat HSCs. Relative protein levels of hepatic fibrosis–related factors regulated by miR-23b/27b/24-1 vs the Puro control. The activation of HSC-T6 cells and primary HSCs was stimulated by pcDNA3.1-CA-ALK5 and TGF-β1, respectively. All results are expressed as the means ± SD (n = 3). $^{*}P < .05$, $^{**}P < .01$.

evidence that the miR-23b/27b/24-1 cluster decreased the severity of liver damage and remarkably attenuated ECM deposition (especially collagen deposition) in the liver of mice with hepatic fibrosis. Our study also showed that the miR-23b/27b/24-1 cluster suppressed 21 ECM proteins, including 16 collagens (type I, III, IV, V, VI, XVII, and XVIII collagens), FBLN5, FN1, LAMβ1, LUM, and MFAP4. Significant protein interactions and protein colocalization and co-expression relationships were identified among the 21 ECM proteins. The miR-23b/27b/24-1 cluster effectively reduced ECM deposition, especially collagen deposition, by activated HSCs and attenuated hepatic fibrosis. In the literature, 7 types of collagens have been reported to be increased during hepatic fibrosis,[5] and we showed that the protein expression of 6 of these collogen genes is down-regulated by the miR-23b/27b/24-1 cluster. The proteins with reduced expression included type I (COLIα1/2), III (COLIIIα1), IV (COLIVα1/2/4/5), V (COLVα1/2/3), VI (COLVIα1/2/3), and XVIII (COLXVIIIα1) collagens. Hepatic fibrosis agonists include TGF-β proteins, ITGs, TIMPs, and LOXs, and hepatic fibrosis antagonists include BMPs and MMPs.[4] In this study, the miR-23b/27b/24-1 cluster directly down-regulated TGF-β2, Gremlin1, ITGα2/5, and LOX protein expression, and all 5 proteins are hepatic fibrosis agonists. The miR-23b/27b/24-1 cluster also indirectly down-regulated the expression of other hepatic fibrosis agonists, such as TGF-β1, CTGF, and TIMP1. At the same time, the cluster did not directly down-regulate the expression of hepatic fibrosis antagonists, such as BMPs and MMPs. Of the 7 possible hepatic fibrosis antagonists with expression suppressed by the miR-23b/27b/24-1 cluster, only MMP8 and MMP19 might be truly related to hepatic fibrosis. Therefore, the miR-23b/27b/24-1 cluster suppresses the expression of many hepatic fibrosis agonists but negligibly influences that of hepatic fibrosis antagonists, resulting in a reduction in ECM deposition.

Enhanced TGF-β signaling or decreased BMP signaling promotes HSC activation and subsequent hepatic fibrosis after liver injury.[8] Gremlin1 is an antagonist of BMPs and is one of the downstream target molecules of the TGF-β signaling pathway. Previous research by our group verified that Gremlin1 promotes HSC activation and hepatic fibrogenesis by impairing BMP signaling and enhancing TGF-β signaling. Knockdown of Gremlin1 expression enhanced BMP signaling and decreased TGF-β signaling.[7,28] In our present study, miR-23b coordinated with miR-27b to down-regulate Gremlin1 expression. The latter miRNA was co-expressed with 16 proteins that are

hepatic fibrosis agonists. In addition, miR-23b directly down-regulated TGF-β2 expression, and the miR-23b/27b/24-1 cluster also suppressed TGF-β1 expression. TGF-β2 was co-expressed with 6 hepatic fibrosis agonists, including COLVI α1, COLVIII α1, FBLN5, ITGα1, ITGβ1, and TGF-β3. In the TGF-β noncanonical pathway, mitogen-activated protein kinases phosphorylate avian erythroblastosis virus E26 oncogene homolog 1 (ETS)1. Then, phosphorylated ETS1 and phosphorylated Smad2/3 cooperatively promote the transcription of *CTGF*.[29,30] CTGF activates mitogen-activated protein kinases by binding integrins (eg, avβ3 and a6β1). Moreover, CTGF enhances TGF-β signaling and suppresses BMP activity.[31,32] Thus, by down-regulating Gremlin1, TGF-β1, and TGF-β2 expression, the miR-23b/27b/24-1 cluster impairs TGF-β signaling and enhances BMP signaling, and the cluster interferes with the crosstalk between TGF-β and CTGF signaling pathway components.

TGF-β proteins can be activated by members of the integrin family that interact with a linear arginine-glycine-–aspartic acid motif in an N-terminal fragment of the TGF-β gene product called *latency-associated peptide*.[33] In this study, miR-27b directly down-regulated ITGα2 and ITGα5 expression. Both ITGα2 and ITGα5 are co-expressed with 2 hepatic fibrosis agonists (ITGβ1 and ITGβ7) and with 8 ECM proteins (COLIα1, COLIα2, COLVIα1, COLVIα2, Fn1, and LAMβ1). Hence, miR-27b inhibits TGF-β activation and decreases ECM secretion through direct down-regulation of ITGα2 and ITGα5 expression.

In hepatic fibrosis, HSCs and portal fibroblasts are major producers of LOX, which promotes HSC activation, enhances ECM stiffness, and limits the degree of fibrosis attenuation.[34] Moreover, LOX is a downstream target of TGF-β, and a stiffer ECM leads to increased TGF-β activation.[35] Our findings show that direct down-regulation of LOX expression was achieved by miR-23b coordinating with miR-24-1. Decreased LOX expression prevents covalent crosslinking in the ECM, and it disrupts the activation of TGF-β triggered by ECM stiffness. Performing module and GeneMANIA analyses, we discovered that LOX was co-expressed with CTGF and TIMP1. Reduced TIMP1 expression induced by the miR-23b/27b/24-1 cluster weakened MMP inhibition, which in turn increased ECM degradation. Accordingly, the miR-23b/27b/24-1 cluster accelerates ECM degradation through down-regulation of LOX and TIMP1 expression.

In summary, the miR-23b/27b/24-1 cluster directly down-regulates TGF-β2, Gremlin1, and ITGα2/5 expression, which decreases ECM synthesis. Furthermore, the miR-23b/27b/24-1 cluster directly down-regulates LOX expression to soften the ECM. Moreover, a reduction in TIMP1 expression resulting from weakened TGF-β signaling promotes ECM degradation. Therefore, ECM synthesis enhancement and ECM degradation impairment in hepatic fibrosis are attenuated by the miR-23b/27b/24-1 cluster because it directly down-regulates TGF-β2, Gremlin1, ITGα2/5, and LOX expression, modulating the expression of other hepatic fibrosis–related genes (Figure 10). For clinical application of the exogenous miR-23b/27b/24-1 cluster, a few obstacles must be overcome. Lentiviral delivery of the miR-23b/27b/24-1 cluster raises safety concerns, and lentiviruses lack specificity. As alternatives to lentiviruses, nanoparticles or micelles synthesized with biologically compatible materials may be used for targeted intracellular drug delivery.[36,37] In addition, the miR-23b/27b/24-1 cluster might cause side effects when enriched in other cells or organs. The miR-23b/27b/24-1 cluster needs to be exclusively delivered and expressed in activated HSCs. Currently, we are screening HSC-specific aptamers using the Cell-SELEX method, and linking them with miRNAs to explore new methods of targeted therapy. Because the endogenous miR-23b/27b/24-1 cluster is not active during fibrosis, its reactivation also can be explored as a strategy to prevent and treat hepatic fibrosis.

Materials and Methods

Plasmid Construction, Cell Culture, and Transfection

Luciferase reporter gene expression plasmids pMIR-Luc-3'UTR and pMIR-Luc-3'UTR-mutant were constructed by inserting full-length 3'UTR and mutant of 10 rat hepatic fibrosis genes into the MCS of pMIR-REPORT Luciferase (pMIR-Luc) plasmid. Lentivirus expression plasmid pCDH-miR-23b/27b/24-1 was constructed by inserting the gene of each miRNA and the cluster into pCDH-CMV-MCS-EF1-Puro plasmid. pCDH-CMV-MCS-EF1-Puro plasmid, with a CMV promoter and a total size of 7384 bp, was purchased from Huayueyang Biological (Beijing, China) Technology Co, Ltd. All primers are synthesized by Sangon Biotech (Shanghai, China) and the primers information is shown in Table 2. Plasmid pcDNA3.1-CA-ALK5 (TGF-β signaling activin receptor-like kinase 5) was as a gift presented by Professor Miyazono at Tokyo University.

The HSC–T6 cell line was maintained in our laboratory and was cultured in high-glucose Dulbecco's modified Eagle medium (DMEM) (Thermo Scientific, Boston, MA) supplemented with 10% newborn calf serum (Thermo Scientific) and 1% penicillin-streptomycin. Cells were seeded in a 6-well plate for Western blot or real-time PCR at a density of 4×10^5 cells per well or in a 24-well plate for luciferase assays at a density of 2×10^4 cells per well in a humidified atmosphere containing 5% CO_2 at 37°C.

The 293FT cell line was a gift from Dr Yun-Hong Zha's group (The People's Hospital, China Three Gorges University) and cultured in high-glucose DMEM supplemented with 10% fetal bovine serum (Thermo Scientific), 0.5 mg/mL G418 (Sigma, Darmstadt, Germany), 1% penicillin-streptomycin, 2 mmol/L L-GlutaMAX (Gibco, Shanghai, China), 0.1 mmol/L modified Eagle medium (MEM) nonessential amino acids (Gibco), and 1 mmol/L sodium pyruvate (Gibco).

HSC-T6 cells were transiently transfected with pMIR-Luc-3'UTR, pMIR-Luc-3'UTR-mutant, and pCDH-miR-23b/27b/24-1 plasmids with TurboFect Transfection Reagent (R0531; Thermo Scientific) according to the manufacturer's instructions. Cells were collected at 24 hours for real-time PCR or luciferase activity, and at 48 hours for Western blot.

The sequences of mature miR-23b-5p/3p, miR-27b-5p/3p, and miR-24-1-5p/3p were from the miRBase (http://

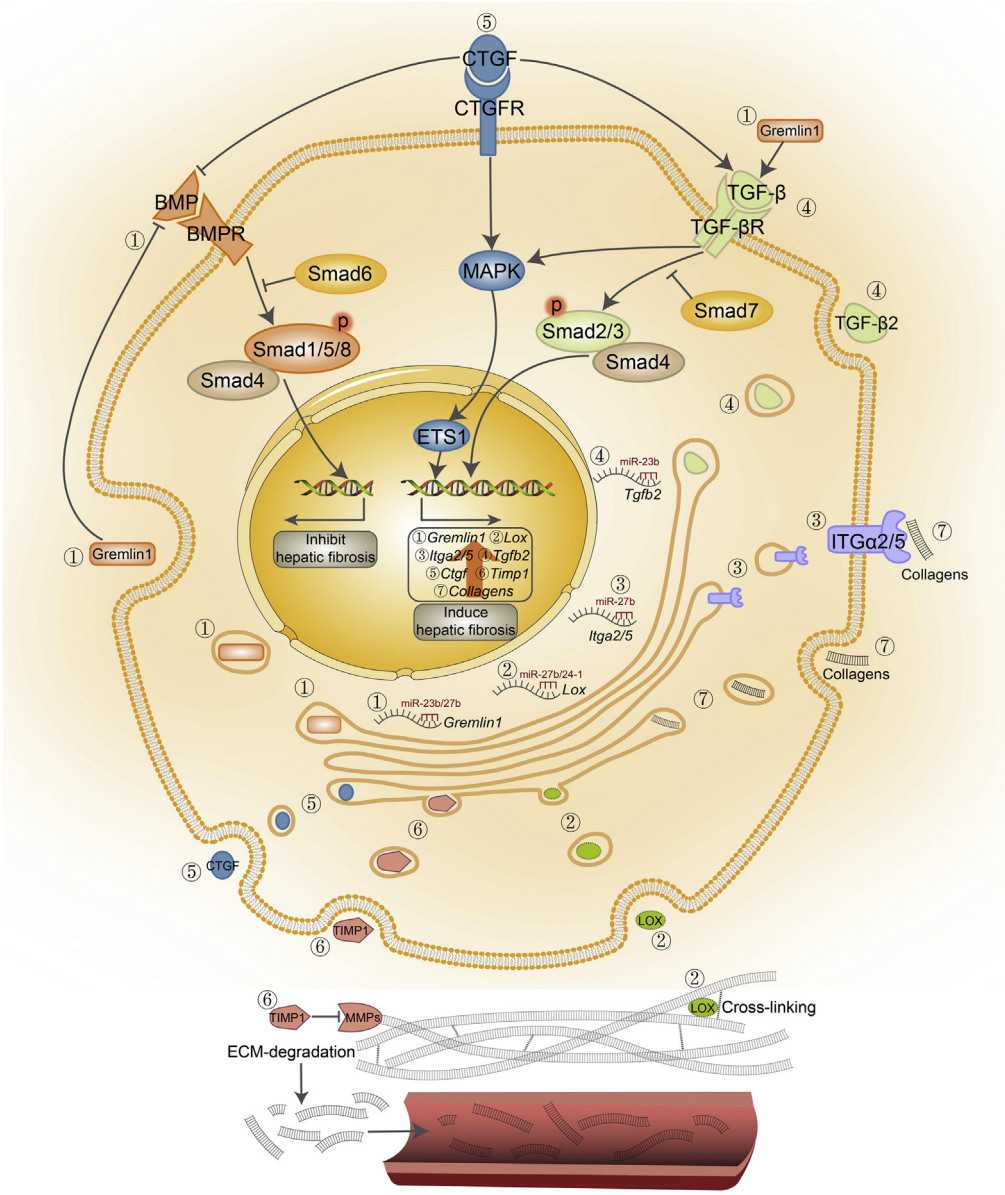

Figure 10. Mechanisms by which the miRNA-23b/27b/24-1 cluster inhibits HSC activation. ① Gremlin1 expression, down-regulation, synthesis, secretion, and related functions. ② LOX expression, down-regulation, synthesis, secretion, and ECM crosslinking. ③ ITG2/5 expression, down-regulation, synthesis, secretion, and binding with collagens. ④ TGF-β2 expression, down-regulation, synthesis, secretion, and promotion of the TGF-β signaling pathway. ⑤ CTGF expression, synthesis, secretion, and related functions. ⑥ TIMP1 expression, synthesis, secretion, and inhibiting MMP expression. ⑦ Collagen expression, synthesis, secretion, and degradation. BMPR, bone morphogenetic protein receptor; CTGFR, connective tissue growth factor receptor; MAPK, mitogen-activated protein kinase.

www.mirbase.org) online server prediction and synthesized by RiboBio Co (Guangzhou, China). Mimic negative control (#22) and fluorescent labeling miRNA mimic also were purchased from RiboBio Co. The transfection details are as previously described[7] and the miRNA mimic information is shown in Table 3.

Lentivirus Packaging and Target Cell Infection

293FT cells were seeded on a 10-cm cell culture plate (Corning, Shanghai, China) the day before transfection. A total of 12 μg plasmids (pLP1, pLP2, pLP/VSVG each 3 μg, and 3 μg pCDH-miR-23b/27b/24-1 or pCDH-Green fluorescent protein) and 36 μL Lipofectamine 2000 (Invitrogen. Shanghai, China) were diluted and gently mixed in 1.5 mL DMEM (no serum, no Penicillin/Streptomycin), respectively. Both diluted plasmids and transfection reagent were incubated separately for 5 minutes at room temperature and then mixed together to incubate for another 20 minutes to form DNA–Lipofectamine 2000 complexes. While the complexes were forming, 293FT cells were being trypsinized and resuspended in 5 mL lentiviral medium (no G418, no P/S), and then the DNA–Lipofectamine 2000 complexes were added to the cell suspension and gently mixed. Cells were incubated overnight at 37°C in a humidified 5% CO_2 incubator, then the medium with fresh lentiviral medium was removed the next day and cells were incubated for another 48 hours. The medium was collected with a syringe and filtered through a 0.45-μm filter to harvest viral supernatants. The viral supernatants were pipetted into a 1.5-mL sterile tube in 1-mL aliquots, and then stored at -80°C. Before use, the virus supernatant is thawed at room temperature, and 2 mL lentiviral medium and 2 mL viral supernatants with 4 μg/mL polybrene (Sigma) were mixed

Table 2. All Primers for Plasmids Construction

Plasmids		Primers
pMIR-Luc-TGF-β2-3'UTR	F	5'-gctgagctcgcctgtacaacaccat-3'
	R	5'-gggacgcgttacagtctgaatgatca-3'
pMIR-Luc-TGF-β2-3'UTR-mutant23b	F	5'-tggaagaatttgttagtgttaattgcctcaggagaaaaaacaaaa-3'
	R	5'-cctgttttgttttgttttttctcctgaggcaattaacactaacaaattc-3'
pMIR-Luc-tgfβr1-3′UTR	F	5'-gatacgcgttgtgcttgaaccactgag-3'
	R	5'-gccaagcttccttccttcacactag-3'
pMIR-Luc-tgfβr2-3′UTR	F	5'-atgacgcgtttcagccagataggac-3'
	R	5'-cggaagcttacctacaagagaccatc-3'
pMIR-Luc-tgfβr2-3'UTR-mutant23b	F	5'-ccatactcatgtattcaaatagggcctcaggtgcacaatactcttt-3'
	R	5'-tgatataaaaagagtattgtgcacctgaggccctatttgaatacatgag-3'
pMIR-Luc-Smad2-3'UTR-1	F	5'-gccacgcgttgtctgtctgtctcatga-3'
	R	5'-ggcaagcttaaatgggcatccgctttc-3'
pMIR-Luc-Smad2-3'UTR-1-mutant27b	F	5'-tagtcagcatagtttctgccagccgcctcagttctgggactgtgtcct-3'
	R	5'-tccagggccaggacacagtcccagaactgaggcggctggcagaaacta-3'
pMIR-Luc-Smad2-3'UTR-2	F	5'-cgcacgcgtgaaaagaggcaacgagat-3'
	R	5'-ggcaagcttcacagagagcaaaggcag-3'
pMIR-Luc-Smad2-3'UTR-2-mutant27b	F	5'-tggtggtcctcagtggctgatccgtgcgcctcagtggagataccaagtg-3'
	R	5'-tacagataacacacttggtatctccactgaggcgcacggatcagccactga-3'
pMIR-Luc-Smad3-3'UTR	F	5'-tatgagctcgatggcctacgcaggtac-3'
	R	5'-gcgacgcgtctatgttctccacagt-3'
pMIR-Luc-Smad3-3'UTR-mutant23b	F	5'-gttccagaggggacaaaagtgcaccctccgcctcagtaaatcttctg-3'
	R	5'-ctggatcatcagaagatttactgaggcggagggtgcacttttgt-3'
pMIR-Luc-G3	F	5′-ttgagctcttgttgcagtctccacct-3′
	R	5′-cccaagctttgcacagaaagaaga-3′
pMIR-Luc-G3-mutant23b	F	5′-gaggaaggatagtttccaccatgtgggcctcaggtaagcaaaagagt-3′
	R	5′-cattaaataaccataactcttttgcttacctgaggcccacatggtgg-3′
pMIR-Luc-G3-mutant27b	F	5′-aggaattctaggtccttcggttgcctcagtttcgaatgttttct-3′
	R	5′-cgtataaaacagagaaagaaaacattcgaaactgaggcaaccgaaggacc-3′
pMIR-Luc-col4α1-3'UTR	F	5'-cgcgtgggtttccaacaccaggccaccgaatgtgaaaacaccagcctttctcactcaca-3'
	R	5'-agcttgtgagtgagaaaggctggtgttttcacattcggtggcctggtgttggaaaccca-3'
pMIR-Luc-col4α1-3'UTR-mutant23b	F	5'-cgcgtgggtttccaacaccaggccaccggcctcaggaacaccagcctttctcactcaca-3'
	R	5'-agcttgtgagtgagaaaggctggtgttcctgaggccggtggcctggtgttggaaaccca-3'
pMIR-Luc-MMP13-3'UTR	F	5'-tgcgagctcggaccatcacagattag-3'
	R	5'-tcgacgcgtcacacatcagtaagcacc-3'
pMIR-Luc-MMP13-3'UTR-mutant27b	F	5'-agtggagatatcaggggagagcttagttgcctcagcaagcttcagtaa-3'
	R	5'-ctcaaagataacttactgaagcttgctgaggcaactaagctctcccc-3'
pMIR-Luc-MMP14-3'UTR	F	5'-cgcgttggagaaccttccaaaggagcctgagccattaaggactaaatgggtctgaggaa-3'
	R	5'-agctttcctcagacccatttagtccttaatggctcaggctcctttggaaggttctccaa-3'
pMIR-Luc-MMP14-3'UTR-mutant24-1	F	5'-cgcgttggagaaccttccaaaggagcgcctcaggttaaggactaaatgggtctgaggaa-3'
	R	5'-agctttcctcagacccatttagtccttaacctgaggcgctcctttggaaggttctccaa-3'
pMIR-Luc-LOX-3'UTR	F	5′-ggcgagctccaccgtattagaaagaagc-3′
	R	5′-cggaagcttgcttggcttatactgtccct-3′
pMIR-Luc-LOX-3'UTR-mutant27b	F	5′-gaccgctgtgaccttacttcaagcctcaggactgtgtgca-3′
	R	5′-atcctactgctgcacacagtcctgaggcttgaagtaagg-3′
pMIR-Luc-LOX-3'UTR-mutant24-1	F	5′-ggcgagctccaccgtattagaaagaagc-3′
	R	5′-ggcgagctccaccgtattagaaagaagc-3′
pMIR-Luc-Itgα2-3′UTR	F	5'-tatacgcgttagggctaggcagggact-3'
	R	5'-gtgaagcttgctgatgtacctcctg-3'
pMIR-Luc-Itgα2-3′UTR-mutant27b	F	5'-gacagtgaaacttgccttttagcctcagggagtaaagacatctaagg-3'
	R	5'-gtcatgaattgaccttagatgtctttactccctgaggctaaaaaggcaagtttc-3'
pMIR-Luc-Itgα5-3′UTR	F	5'-tatgagctctgagccctcctgatctca-3'
	R	5'-tatacgcgtgtgagtggggtttattgc-3'

Table 2. Continued

Plasmids		Primers
pMIR-Luc-Itgα5-3′UTR-mutant27b	F	5’-aagcttgtggatccttccccccacgcgcctcagtggaccctcgtttac-3’
	R	5’-tgagagggcatgtgtaaacgagggtccactgaggcgcgtgggggggaag-3’
pCDH-miR-23b/27b/24-1	F	5′-cgtgaattcgtgtccccagggttaaag-3′
	R	5′-ataggatcccgctcggcttctgctctg-3′
pCDH-miR-23b	F	5′-cgtgaattcgtgtccccagggttaaag-3′
	R	5′-tcaggatcccatcgccggccataatta-3′
pCDH-miR-27b	F	5′-aatgaattcctcctgcagaaccgtggc-3′
	R	5′-gctggatccctgtaggcacatttaagg-3′
pCDH-miR-24-1	F	5′-ccggaattcatgtcttcacagtcgctg-3′
	R	5′-aatggatcccgactcctgttcctgctg-3′

F, forward; R, reverse.

together to infect target cells, second round of infection 24 hour later and split target cells to culture plate with fresh target growth medium.

Luciferase Reporter Assay

HSC-T6 cells were seeded in 24-well culture plates (Corning) at a density of 2×10^4 cells per well 1 day before transfection. Each reporter construction and its mutant were co-transfected with miR-23b, miR-27b, miR-24-1 mimic, or a negative control mimic to confirm the direct binding effect of miR-23b/27b/24-1 cluster on 3’UTR of profibrotic genes. After 24 hours of transfection, all cells were collected by centrifugation at 1000 rpm for 5 minutes at 4°C and lysed in cell lysis buffer (Promega, Beijing, China) for 20 minutes on ice, and then the supernatant was transferred to a sterile tube after centrifugation at 12,000 rpm for 10 minutes at 4°C. The total protein concentrations were measured with the BCA Protein Assay kit (Thermo Scientific). Luciferase activities were performed with the Luciferase Assay System (Promega) according to the manufacturer’s instructions and measured with a fluorescence detector (Brethold, Bad Wildbad, Germany).

Isolation and Culture of Primary Rat HSCs

The use of animals for this study was approved by the laboratory animal center of China, Three Gorges University. Primary rat HSCs were isolated from 12-week-old, 400–500 g male Sprague Dawley rats by in situ pronase, collagenase perfusion, and OptiPrep gradient centrifugation using a described method with minor modifications.[34] Freshly isolated HSCs were cultured in high-glucose DMEM (Invitrogen, Shanghai, China) containing 10% fetal bovine serum and 1% penicillin-streptomycin on 6-well plates at 37°C in a humidified 5% CO_2 incubator. After HSCs completely adhered, 10 ng/mL TGF-β protein (Sino Biological, Beijing, China) was used to stimulate their activation for 72 hours. In subsequent lentiviral infection assay, the activated HSCs were infected with pCDH-miR-23b/27b/24-1 lentivirus granule. After another 48 hours of culture, the cells were digested, collected for Western blot analysis, or sent to BGI (Shenzhen, China) for transcriptome high-throughput sequencing.

RNA Extraction and Real-Time PCR

HSC-T6 cells were harvested 24 hours after being transfected with pCDH-miR-23b/27b/24-1, total microRNAs were isolated with the miRcute miRNA Extraction Kit (DP501; TIANGEN, Beijng, China), reverse transcription of complementary DNA was performed with the miRcute miRNA complementary DNA Synthesized Kit (KR201; TIANGEN), and real-time PCR was performed using the miRcute miRNA Quantitation Kit (FP401; TIANGEN) on a Multivariate Quantitative PCR system (CFD-3220; BIO-RAD, Shanghai, China) according to the manufacturer’s protocols.

Table 3. All miRNA Mimic Sequences

Species	miRNAs	Serial number of miRBase	Sequence of mature miRNAs
Rat	rno-miR-23b-5p	MIMAT0017099	GGGUUCCUGGCAUGCUGAUUU
Rat	rno-miR-23b-3p	MIMAT0000793	AUCACAUUGCCAGGGAUUACC
Rat	rno-miR-27b-5p	MIMAT0017101	AGAGCUUAGCUGAUUGGUGAACAG
Rat	rno-miR-27b-3p	MIMAT0000798	UUCACAGUGGCUAAGUUCUGC
Rat	rno-miR-24-1-5p	MIMAT0003153	GUGCCUACUGAGCUGAUAUCAG
Rat	rno-miR-24-1-3p	MIMAT0000794	UGGCUCAGUUCAGCAGGAACAG
Rat	Negative control	micrONTM miRNA mimic Ncontrol #22_standard	
Rat	Fluorescent labeling	micrONTM mimics negative control #22(5Cy3)	

Table 4. Real-Time PCR Primers for miR-23b, miR-27b, miR-24-1, and U6

Genes, name	Primer sequence, item number
miR-23b-5p	F SSD809230953 R SSD089261711
miR-23b-3p	F MIR8002134 R SSD089261711
miR-27b-5p	F SSD1342492802 R SSD089261711
miR-27b-3p	F SSD809230959 R SSD089261711
miR-24-1-5p	F SSD1373111211 R SSD089261711
miR-24-1-3p	F SSD809230954 R SSD089261711
U6	F 5′-ctcgcttcggcagcaca-3′ R 5′-aacgcttcacgaatttgcgt-3′

F, forward; R, reverse.

U6 was used as a housekeeping gene to normalize the quantification of total microRNAs and experiments were analyzed with Opticon Monitor 3 software (BIO-RAD, Shanghai, China). Statistical analysis was performed with GraphPad Prism 8.0 software (GraphPad Software, San Diego, CA) to analyze the relative expression level of each miRNA on at least 3 biologic repeats. The primers were purchased from TIANGEN and are listed in Table 4.

Transcriptomic Analysis Using RNA-seq

For the transcriptomic analysis, mRNA was isolated from the cultured cells using the TRIzol RNA extraction reagent (Invitrogen. Shanghai, China). Equal amounts of mRNA from 3 independent preparations were pooled, and the library then was constructed using the BGISEQ500 platform (BGI). The RNA-seq data were first processed by filtering the adaptor sequences and removing the low-quality reads using SOAPnuke (v1.5.2)[35] to obtain clean reads. The clean reads were mapped to the reference genome using HISAT2 (v2.0.4; http://www.ccb.jhu.edu/software/hisat/index.shtml).[36] Bowtie2 (v2.2.5)[37] was applied to align the clean reads to the reference coding gene set, then the expression level of the gene was calculated by RSEM (v1.2.12).[38] Reads per kilobases per million reads were used to evaluate the RNA abundance. The value of the reads per kilobases per million reads of 1 or greater was defined as a cut-off value for an identified gene. The heatmap was drawn by pheatmap (v1.0.8)[39]according to the gene expression in different samples. Essentially, differential expression analysis was performed using DESeq (v1.34.1),[40] with a Q value of 0.05 or less. To discover the mechanisms underlying phenotypic change, GO (http://www.geneontology.org) and KEGG (https://www.kegg.jp) enrichment analysis of annotated different expressed genes was performed by Phyper (https://en.wikipedia.org/wiki/Hypergeometric_distribution) based on the Hyper geometric test. The significant levels of terms and pathways were corrected by P value with a rigorous threshold ($P \leq .05$) by Bonferroni.[41] The information from PPIs were collected by the Search Tool for the Retrieval of Interacting Genes (STRING, version 11.0; http://string-db.org).[42] An interaction score of 0.4 or greater was used as evaluation criteria in the PPI network. In addition, Cytoscape software (version 3.7.1; http://www.cytoscape.org) was used for constructing the PPI network. MCODE was used to analyze PPI network modules, and degree cut-off value of 2 or greater, node score cut-off value of 2 or greater, K-core of 2 or greater, and a maximum depth of 100 were used as the default parameters to set it to the cut-off condition. Finally, CytoHubba, a Cytoscape plugin, was used to explore PPI network hub genes.[43] GeneMANIA (http://www.genemania.org) was used to display gene networks and predict gene function.

Table 5. Primary Antibodies and Secondary Antibodies for Western Blot Assay

Primary antibody	Dilution ratio	Company	Secondary antibody	Dilution ratio	Company
TGF-β1	1:1000	Santa Cruz (Dallas, TX)	HRP-labeled goat anti-rabbit IgG	1:3000	NovoGene (Beijing, China)
TGF-β2	1:800	Santa Cruz	HRP-labeled goat anti-mouse IgG	1:5000	NovoGene
Smad3	1:800	Santa Cruz	HRP-labeled rabbit anti-goat IgG	1:12,000	NovoGene
Gremlin1	1:800	Santa Cruz	HRP-labeled rabbit anti-goat IgG	1:12,000	NovoGene
Collagen Iα1	1:800	Santa Cruz	HRP-labeled rabbit anti-goat IgG	1:12,000	NovoGene
Collagen Iα2	1:800	Santa Cruz	HRP-labeled rabbit anti-goat IgG	1:12,000	NovoGene
LOX	1:800	Santa Cruz	HRP-labeled goat anti-mouse IgG	1:5000	NovoGene
ITGα2	1:800	Santa Cruz	HRP-labeled goat anti-mouse IgG	1:5000	NovoGene
ITGα5	1:800	Santa Cruz	HRP-labeled goat anti-mouse IgG	1:5000	NovoGene
MMP2	1:800	Santa Cruz	HRP-labeled goat anti-mouse IgG	1:5000	NovoGene
MMP9	1:800	Santa Cruz	HRP-labeled goat anti-mouse IgG	1:5000	NovoGene
TIMP1	1:800	Santa Cruz	HRP-labeled goat anti-mouse IgG	1:5000	NovoGene
β-actin	1:3000	Santa Cruz	HRP-labeled goat anti-mouse IgG	1:5000	NovoGene

HRP, horseradish peroxidase.

Western Blot Analysis

For protein expression analysis, transfected cells were washed with cold phosphate-buffered saline and lysed in cell lysis buffer (Promega) with protease inhibitor cocktail for 30 minutes on ice. The cell lysate was centrifuged at 12,000 rpm for 20 minutes at 4°C and the supernatants were collected. The total protein concentration was quantified using the Pierce BCA Protein Assay Kit (Thermo Scientific). An equal amount of total protein from each sample was subjected to 12% sodium dodecyl sulfate–polyacrylamide gel electrophoresis separation and transferred onto a polyvinylidene difluoride membrane on ice. The blots were blocked with 5% nonfat milk and 0.1% Tween 20 at room temperature for 1 hour and then incubated with diluted primary antibodies overnight at 4°C. Followed by Tris Buffered Saline with Tween (TBST) buffer washing, the membranes were incubated with the secondary antibodies for 50 minutes at room temperature and then measured with the enhanced chemiluminescence detection kit (Thermo) according to the manufacturer's instructions. The chemiluminescence on the membrane was detected using the Bioshine Chemi Q 4800mini Capture system (Qinxiang, Shanghai, China). Densitometric analyses of the band intensities were performed using KODAK Molecular Imaging Software (Eastman Kodak Company). All primary and secondary antibodies as well as dilution ratios are listed in Table 5.

Mice and Fibrosis Induction

Hepatic fibrosis was induced using CCl_4 (Macklin, Shanghai, China) dissolved in olive oil. Six-week-old male C57BL/6 mice (body weight, 20 g) were purchased from China Three Gorges University Laboratory Animal Center and assigned randomly to a mock group, CCl_4 group, LV-PURO+CCl_4 group, or LV-miR-23b/27b/24-1+CCl_4 group. The mice were administered pCDH-miR-23b/27b/24-1 (dose of 3×10^7 transducing unit (TU) for the LV-miR-23b/27b/24-1+CCl_4 group), pCDH-Puro (an inactive analogue for the group LV-PURO+CCl_4), or saline (for the mock and CCl_4 groups) by tail intravenous injection 3 times per week, starting on day 1, and the mice were challenged with intraperitoneal injections of CCl_4 three times per week (the first dose was 0.25 mL/kg body weight, followed by 0.5 mL/kg), starting on day 8. Mock group mice received olive oil in lieu of CCl_4 injections. The mice were killed on day 63, and the livers were removed for histologic observation. The mice were housed in the China Three Gorges University Laboratory Animal Center and maintained according to the institution's guidelines. All animal experiments were approved by the China Three Gorges University Committee on Laboratory Animal Ethics.

Histology Staining and TPEF/SHG Analyses

The pathologist (L.H.) processed paraffin-embedded tissue sections for H&E staining and Masson's trichrome blue staining for collagen following standard procedures. Paraffin-embedded tissue sections were delivered to Hangzhou Chou-Tu Technology Company (Hangzhou, China) for TPEF/SHG analyses. The slides were numbered and disordered (by L.H.), and then scored (Y.-R.N.) in a blinded fashion. The Scheuer scoring system was used to evaluate fibrosis and necroinflammatory activity. A total of 100 parameters were measured as continuous variables relative to their original dimensions in TPEF/SHG analyses, including the total collagen percentage, aggregated collagen percentage, distributed collagen percentage, number of strings, number of short strings, number of long strings, number of thin strings, number of thick strings, string area, string length, string width, string eccentricity, string in solidity, string perimeter, string orientation, number of crosslinks, and so forth.

The Predictor-WJF Algorithm

Predictor-WJF has been designed to identify miRNA targets. It incorporates 5 independent computational target prediction algorithms (Targetscan,[44] miRDB,[45] micro-CDS,[46] miRanda,[47] and PicTar[48]) and 1 data set of experimentally validated miRNA targets (ENCORI[49]). A flowchart of this pipeline is shown in Figure 4*C*. Each gene predicted as a target of a miRNA by any of the 6 data sources is assigned a score (with values of 1 for each computational algorithm and 2 for ENCORI). The final score for a gene is calculated by the sum of the score for each data set. The output of the pipeline is a list of target genes scored and ranked.

Statistical Analysis

Data are expressed as the means ± SD. A 2-tailed Student *t* test was performed to compare differences between 2 groups. One-way analysis of variance comparisons were performed to compare differences between 3 or more groups, all data were analyzed with GraphPad Prism 8.0 Software, and $P < .05$ was considered to be statistically significant. Each experiment was performed with at least 3 biological repeats.

References

1. Lee UE, Friedman SL. Mechanisms of hepatic fibrogenesis. Best Pract Res Clin Gastroenterol 2011; 25:195–206.
2. Yin C, Evason KJ, Asahina K, Stainier DY. Hepatic stellate cells in liver development, regeneration, and cancer. J Clin Invest 2013;123:1902–1910.
3. Kocabayoglu P, Friedman SL. Cellular basis of hepatic fibrosis and its role in inflammation and cancer. Front Biosci (Schol Ed) 2013;5:217–230.
4. Ding N, Yu RT, Subramaniam N, Sherman MH, Wilson C, Rao R, Leblanc M, Coulter S, He M, Scott C, Lau SL, Atkins AR, Barish GD, Gunton JE, Liddle C, Downes M, Evans RM. A vitamin D receptor/SMAD genomic circuit gates hepatic fibrotic response. Cell 2013;153:601–613.
5. Karsdal MA, Daniels SJ, Holm Nielsen S, Bager C, Rasmussen DGK, Loomba R, Surabattula R, Villesen IF, Luo Y, Shevell D, Gudmann NS, Nielsen MJ, George J, Christian R, Leeming DJ, Schuppan D. Collagen biology

and non-invasive biomarkers of liver fibrosis. Liver Int 2020;40:736–750.
6. Nolan K, Thompson TB. The DAN family: modulators of TGF-beta signaling and beyond. Protein Sci 2014; 23:999–1012.
7. Zeng XY, Zhang YQ, He XM, Wan LY, Wang H, Ni YR, Wang J, Wu JF, Liu CB. Suppression of hepatic stellate cell activation through downregulation of gremlin1 expression by the miR-23b/27b cluster. Oncotarget 2016;7:86198–86210.
8. Kinoshita K, Iimuro Y, Otogawa K, Saika S, Inagaki Y, Nakajima Y, Kawada N, Fujimoto J, Friedman SL, Ikeda K. Adenovirus-mediated expression of BMP-7 suppresses the development of liver fibrosis in rats. Gut 2007;56:706–714.
9. Takada Y, Ye X, Simon S. The integrins. Genome Biol 2007;8:215.
10. Hintermann E, Christen U. The many roles of cell adhesion molecules in hepatic fibrosis. Cells 2019;8:1503.
11. Roeb E. Matrix metalloproteinases and liver fibrosis (translational aspects). Matrix Biol 2018; 68–69:463–473.
12. Ren JJ, Huang TJ, Zhang QQ, Zhang HY, Guo XH, Fan HQ, Li RK, Liu LX. Insulin-like growth factor binding protein related protein 1 knockdown attenuates hepatic fibrosis via the regulation of MMPs/TIMPs in mice. Hepatobiliary Pancreat Dis Int 2019;18:38–47.
13. Geach TJ, Dale L. Members of the lysyl oxidase family are expressed during the development of the frog Xenopus laevis. Differentiation 2005;73:414–424.
14. Chen W, Yang A, Jia J, Popov YV, Schuppan D, You H. Lysyl oxidase (LOX) family members: rationale and their potential as therapeutic targets for liver fibrosis. Hepatology 2020;72:729–741.
15. Ikenaga N, Peng ZW, Vaid KA, Liu SB, Yoshida S, Sverdlov DY, Mikels-Vigdal A, Smith V, Schuppan D, Popov YV. Selective targeting of lysyl oxidase-like 2 (LOXL2) suppresses hepatic fibrosis progression and accelerates its reversal. Gut 2017;66:1697–1708.
16. Lee YA, Wallace MC, Friedman SL. Pathobiology of liver fibrosis: a translational success story. Gut 2015; 64:830–841.
17. Wang Y, Luo J, Zhang H, Lu J. microRNAs in the same clusters evolve to coordinately regulate functionally related genes. Mol Biol Evol 2016;33:2232–2247.
18. Yuan X, Liu C, Yang P, He S, Liao Q, Kang S, Zhao Y. Clustered microRNAs' coordination in regulating protein-protein interaction network. BMC Syst Biol 2009;3:65.
19. Fukumoto I, Koshizuka K, Hanazawa T, Kikkawa N, Matsushita R, Kurozumi A, Kato M, Okato A, Okamoto Y, Seki N. The tumor-suppressive microRNA-23b/27b cluster regulates the MET oncogene in oral squamous cell carcinoma. Int J Oncol 2016;49:1119–1129.
20. Nishida K, Kuwano Y, Rokutan K. The microRNA-23b/27b/24 cluster facilitates colon cancer cell migration by targeting FOXP2. Cancers (Basel) 2020;12:174.
21. Rogler CE, Levoci L, Ader T, Massimi A, Tchaikovskaya T, Norel R, Rogler LE. MicroRNA-23b cluster microRNAs regulate transforming growth factor-beta/bone morphogenetic protein signaling and liver stem cell differentiation by targeting Smads. Hepatology 2009;50:575–584.
22. Wang Y, Vincent R, Yang J, Asgharpour A, Liang X, Idowu MO, Contos MJ, Daitya K, Siddiqui MS, Mirshahi F, Sanyal AJ. Dual-photon microscopy-based quantitation of fibrosis-related parameters (q-FP) to model disease progression in steatohepatitis. Hepatology 2017;65:1891–1903.
23. Wang Y, Huang W, Li R, Yun Z, Zhu Y, Yang J, Liu H, Liu Z, Feng Q, Hou J. Systematic quantification of histological patterns shows accuracy in reflecting cirrhotic remodeling. J Gastroenterol Hepatol 2017; 32:1631–1639.
24. Tsuchida T, Friedman SL. Mechanisms of hepatic stellate cell activation. Nat Rev Gastroenterol Hepatol 2017; 14:397–411.
25. Dijk FV, Olinga P, Poelstra K, Beljaars L. Targeted therapies in liver fibrosis: combining the best parts of platelet-derived growth factor BB and interferon gamma. Front Med (Lausanne) 2015;2:72.
26. Chen ZJ, Liu H, Jain A, Zhang L, Liu C, Cheng K. Discovery of aptamer ligands for hepatic stellate cells using SELEX. Theranostics 2017;7:2982–2995.
27. Rogler CE, Matarlo JS, Kosmyna B, Fulop D, Rogler LE. Knockdown of miR-23, miR-27, and miR-24 alters fetal liver development and blocks fibrosis in mice. Gene Expr 2017;17:99–114.
28. Zhang YQ, Wan LY, He XM, Ni YR, Wang C, Liu CB, Wu JF. Gremlin1 accelerates hepatic stellate cell activation through upregulation of TGF-beta expression. DNA Cell Biol 2017;36:603–610.
29. Zhang YE. Non-Smad signaling pathways of the TGF-beta family. Cold Spring Harb Perspect Biol 2017;9: a022129.
30. Geisinger MT, Astaiza R, Butler T, Popoff SN, Planey SL, Arnott JA. Ets-1 is essential for connective tissue growth factor (CTGF/CCN2) induction by TGF-beta1 in osteoblasts. PLoS One 2012;7:e35258.
31. Abreu JG, Ketpura NI, Reversade B, De Robertis EM. Connective-tissue growth factor (CTGF) modulates cell signalling by BMP and TGF-beta. Nat Cell Biol 2002; 4:599–604.
32. Yosimichi G, Nakanishi T, Nishida T, Hattori T, Takano-Yamamoto T, Takigawa M. CTGF/Hcs24 induces chondrocyte differentiation through a p38 mitogen-activated protein kinase (p38MAPK), and proliferation through a p44/42 MAPK/extracellular-signal regulated kinase (ERK). Eur J Biochem 2001;268:6058–6065.
33. Henderson NC, Arnold TD, Katamura Y, Giacomini MM, Rodriguez JD, McCarty JH, Pellicoro A, Raschperger E, Betsholtz C, Ruminski PG, Griggs DW, Prinsen MJ, Maher JJ, Iredale JP, Lacy-Hulbert A, Adams RH, Sheppard D. Targeting of αv integrin identifies a core molecular pathway that regulates fibrosis in several organs. Nat Med 2013;19:1617–1624.
34. Mederacke I, Dapito DH, Affo S, Uchinami H, Schwabe RF. High-yield and high-purity isolation of hepatic stellate cells from normal and fibrotic mouse livers. Nat Protoc 2015;10:305–315.

35. Li R, Li Y, Kristiansen K, Wang J. SOAP: short oligonucleotide alignment program. Bioinformatics 2008; 24:713–714.
36. Kim D, Langmead B, Salzberg SL. HISAT: a fast spliced aligner with low memory requirements. Nat Methods 2015;12:357–360.
37. Langmead B, Salzberg SL. Fast gapped-read alignment with Bowtie 2. Nat Methods 2012;9:357–359.
38. Li B, Dewey CN. RSEM: accurate transcript quantification from RNA-seq data with or without a reference genome. BMC Bioinformatics 2011;12:323.
39. Kolde R. Package 'pheatmap'. 2019. Available from: https://cran.r-project.org/web/packages/pheatmap/index.html. Accessed May 2, 2020.
40. Wang L, Feng Z, Wang X, Wang X, Zhang X. DEGseq: an R package for identifying differentially expressed genes from RNA-seq data. Bioinformatics 2010;26:136–138.
41. Curtin F, Schulz P. Multiple correlations and Bonferroni's correction. Biol Psychiatry 1998;44(8):775–777.
42. Szklarczyk D, Gable AL, Lyon D, Junge A, Wyder S, Huerta-Cepas J, Simonovic M, Doncheva NT, Morris JH, Bork P, Jensen LJ, Mering CV. STRING v11: protein-protein association networks with increased coverage, supporting functional discovery in genome-wide experimental datasets. Nucleic Acids Res 2019;47:D607–D613.
43. Shannon P, Markiel A, Ozier O, Baliga NS, Wang JT, Ramage D, Amin N, Schwikowski B, Ideker T. Cytoscape: a software environment for integrated models of biomolecular interaction networks. Genome Res 2003; 13:2498–2504.
44. Agarwal V, Bell GW, Nam JW, Bartel DP. Predicting effective microRNA target sites in mammalian mRNAs. Elife 2015;4:e05005.
45. Chen Y, Wang X. miRDB: an online database for prediction of functional microRNA targets. Nucleic Acids Res 2020;48:D127–D131.
46. Paraskevopoulou MD, Georgakilas G, Kostoulas N, Vlachos IS, Vergoulis T, Reczko M, Filippidis C, Dalamagas T, Hatzigeorgiou AG. DIANA-microT web server v5.0: service integration into miRNA functional analysis workflows. Nucleic Acids Res 2013;41:W169–W173.
47. Wang S, Kim J, Jiang X, Brunner SF, Ohno-Machado L. GAMUT: GPU accelerated microRNA analysis to uncover target genes through CUDA-miRanda. BMC Med Genomics 2014;7(Suppl 1):S9.
48. Krek A, Grün D, Poy MN, Wolf R, Rosenberg L, Epstein EJ, MacMenamin P, da Piedade I, Gunsalus KC, Stoffel M, Rajewsky N. Combinatorial microRNA target predictions. Nat Genet 2005;37:495–500.
49. Li JH, Liu S, Zhou H, Qu LH, Yang JH. starBase v2.0: decoding miRNA-ceRNA, miRNA-ncRNA and protein-RNA interaction networks from large-scale CLIP-Seq data. Nucleic Acids Res 2014;42:D92–D97.
50. Scheuer PJ. Classification of chronic viral hepatitis: a need for reassessment. J Hepatol 1991;13(3):372–374.

Received October 4, 2021. Accepted January 19, 2022.

Correspondence
Address correspondence to: Prof Yan-Qiong Zhang, or Prof Jiang-Feng Wu, Medical College, China Three Gorges University, Yichang, Hubei, 443002, China. e-mail: zhangyanqiong@ctgu.edu.cn or wujiangfeng@ctgu.edu.cn; fax: (0086) 07176397328.

Acknowledgments
The authors thank Dr Yan Ren, BGI (Shenzhen, China) for RNA-seq, Professor Miyazono at Tokyo University for offering Plasmid pcDNA3.1-CA-ALK5; Dr Yun-Hong Zha at The People's Hospital of China Three Gorges University for offering the 293FT cell line, Hangzhou Chou-Tu Technology Company for TPEF/SHG analysis, and Shan-Bing Yin for English language polishing.

CRediT Authorship Contributions
Lin-Yan Wan (Data curation: Equal; Formal analysis: Equal; Investigation: Equal; Writing – original draft: Lead)
Hu Peng (Data curation: Equal; Investigation: Equal; Writing – original draft: Equal)
Yi-Ran Ni (Data curation: Supporting; Investigation: Equal; Writing – original draft: Supporting; Writing – review & editing: Equal)
Xue-Ping Jiang (Data curation: Equal; Investigation: Equal)
Jiao-Jiao Wang (Formal analysis: Supporting; Software: Equal; Visualization: Lead)
Yan-Qiong Zhang (Conceptualization: Supporting; Funding acquisition: Supporting; Project administration: Lead; Supervision: Lead)
Lan Ma (Data curation: Supporting; Formal analysis: Supporting; Project administration: Supporting; Visualization: Supporting)
Rui Li (Data curation: Supporting; Methodology: Supporting)
Lin Han (Methodology: Supporting)
Yong Tan (Data curation: Supporting; Formal analysis: Supporting)
Jun-Ming Li (Project administration: Supporting; Resources: Supporting)
Wen-Li Cai (Software: Supporting; Validation: Supporting)
Wen-Fang Yuan (Data curation: Supporting; Formal analysis: Supporting)
Jia-Jie Liang (Data curation: Supporting)
Lu Huang (Data curation: Supporting)
Xu Wu (Data curation: Supporting)
Quan Zhou (Software: Supporting)
Qi-Ni Cheng (Validation: Supporting)
Xue Yang (Validation: Supporting)
Meng-Yuan Liu (Validation: Supporting)
Wen-Bing Ai (Project administration: Supporting; Supervision: Supporting)
Chang-Bai Liu (Project administration: Supporting; Supervision: Supporting)
Hongbing Zhang (Project administration: Supporting; Supervision: Supporting)
Jiang-Feng Wu (Conceptualization: Lead; Funding acquisition: Lead; Writing – review & editing: Lead)

Conflicts of interest
The authors disclose no conflicts.

Funding
Supported by the National Natural Science Foundation of China (81670555, 81200307, and 81800550); the State Key Laboratory Special Fund (2060204); Health Commission of Hubei Province Scientific Research Project (WJ2019H533); and The Opening Foundation of Hubei Key Laboratory of Tumor Microenvironment and Immunotherapy (2019KZL05).